Differentiated endothelial cell behavior in a flow channel microfluidic system

Thesis submitted in partial fulfillment of the requirements for the degree of
Master of Science in Engineering at the University of Applied Sciences
Technikum Wien - Degree Program Tissue Engineering and Regenerative Medicine

By: Garazi Monzo Contreras, BSc
Student Number: 1410692001

Supervisor 1: Ludivine Challet Meylan, PhD
Supervisor 2: Wolfgang Holnthoner, Mag. Dr.

Cambridge, 01/09/2016

FACHHOCHSCHULE
TECHNIKUM WIEN

Declaration

„I confirm that this thesis is entirely my own work. All sources and quotations have been fully acknowledged in the appropriate places with adequate footnotes and citations. Quotations have been properly acknowledged and marked with appropriate punctuation. The works consulted are listed in the bibliography. This paper has not been submitted to another examination panel in the same or a similar form, and has not been published. I declare that the present paper is identical to the version uploaded."

Place, Date

Signature

Abstract

The cardiovascular system is one of the most complex and important systems of the body composed of heart, blood and blood vessels. The inner layer of blood vessels consists of endothelial cells (ECs) which are constantly exposed to shear stress created by the blood flow. Cardiovascular diseases (CVD) are a group of disorders affecting the vascular system and causing 30% of all deaths worldwide. Human disease models enable the understanding of cellular and molecular mechanisms of diseases to develop more efficient treatments. The use of human pluripotent stem cells (hPSCs) to model human disorders have been enhanced with the emergence of two recent techniques: pluripotent stem cell differentiation and genome engineering. In order to better understand the mechanisms underlying CVD, in this study CRISPR/Cas9 knockouts for CCL7 were designed, a novel differentiation technique was employed as well as a microfluidic system was constructed to investigate the role of shear stress in pro-inflammatory protein production, the expression of endothelial adhesion molecules, and vascular constrictor factors related to coagulation-fibrinolysis. CCL7 gene knockout was generated but experiments failed during expansion. Immunofluorescence for PECAM-1, VE-Cadherin and vWF and angiogenesis assay performed in differentiated iPSCs confirmed that these cells behave similarly to primary ECs. Finally, human coronary artery endothelial cells (HCAECs) were cultured under different shear stress intensities (0.06 Pa, 0.3 Pa, 0.6 Pa and 1.2 Pa) and tested for gene expression. Given that the pro-inflammatory mRNA expression levels in primary ECs were upregulated in 0.6 Pa condition. We could hypothesize that 0.6 Pa is the key stress hydrodynamic flow in ECs. In conclusion, the designed microfluidic chamber system using 0.6 Pa offers a new tool for CVD modeling.

Keywords: Endothelial cells, Shear stress, CRISPR/Cas9, differentiation, HCAEC, CCL7

Acknowledgements

"It is beyond a doubt that all our knowledge begins with experience"
-Immanuel Kant

And I owe my most significant research experience to Chad Cowan, the PI that welcomed me into his laboratory and gave me the opportunity to do my master thesis in his lab.

I have to express my sincerest gratitude to my supervisor Dr. Ludivine Challet Meylan, whom I admire for her dedication, her input and great patience. She always had wise words to guide me in the right direction. She taught me the importance of time management and planning.

This project would not have been possible without the contribution of Luke MacQueen, from the Wyss institute, who lend me all the material to do my shear stress experiments and designed the chambers for me.

The Cowan and Strominger lab members had a big influence on this work. They all made me feel so welcome. I would like to mention the technician Yulei Xia, who thought me molecular biology techniques and was always ready to help me interpret my results. The lab manager Jennifer Shay always kept the lab in order very efficiently so that I could work smoothly. The PhD student Max Friesen, for donating his AKT2 cell clones to me and for helping me with his feedback. I would also like to thank the rest of lab members and undergrad students that contributed towards a great work environment: Ben Pope, Carolyn Hudak, Curtis Warren, Haojie Yu, Kruti Vora, Stanley Tam, Takafumi Toyohara, Tørsten Meissner, Xiao Han, Leonardo Ferreira, Paul Franco, Min Jin Lee, Theresa Bandstetter, William Haoudi, Ester Leno Duran and Anita van der Zwan. Last but not least, my co-workers and friends Umji Lee and Alana Allen, for giving me moral support during the tough times and making me a bit less stressed.

I want to thank the University of Applied Sciences Technikum Wien, for giving me the opportunity to do my master thesis abroad as well as the Austrian Marshall Plan Foundation for the funding of my studies abroad.

The friends that I made in Boston contributed to this paper in an indirect way by helping me adapt and making me feel at home. Specially Iratxe Tapia Jara, who has become an important cornerstone in my life.

Finally, I would have not come so far without the support of my parents, who taught me that nothing is impossible and there is always a way to achieve my dreams.

Table of Contents

1 Introduction

The cardiovascular system is one of the most complex and important systems of the body. It is composed of the heart and blood vessels, which are joined to form a closed circuit through which blood flows (WHO, 2016).

The heart is a muscular structure with four cavities therein, two upper known as atria and two lower called ventricles, connected by a valve system and a pump that acts as a pacemaker capable of generating electrical activity which results in contraction rhythm (the systole (contraction) and diastole (relaxation) movements) of the atria and the ventricles to pump blood through the system (Silverthorn, 2007). The blood leaves the heart through the arteries. The largest artery, the aorta, carries blood to most of the body, while the pulmonary artery leads to the lungs for oxygenation. The blood returns to the heart through the vena cava and pulmonary veins (Silverthorn, 2007).

With each beat, the heart pushes a volume of blood into the aorta, this large blood vessel divides into a number of branches directed to every organ. As the vessels divide, these have a decreased diameter. The smallest vessels are the capillaries which are microscopic. These vessels begin to increase their diameter becoming veins that are gathering to form the caval vein leading to the heart (Silverthorn, 2007).

The main function of the cardiovascular system is the transport of blood within the body to every cell in every tissue. The blood transports oxygen from the lungs to the tissues and collects the respiratory waste product carbon dioxide, which is filtered through the kidney and returns to the lungs. Moreover, it transports white blood cells, hormones and all kinds of nutrients to allow a proper function of the body (Silverthorn, 2007).

1.1 Cardiovascular physiology

The circulatory system is divided into systemic, pulmonary and coronary circulation:

- in the systemic circulation blood is pumped from the left ventricle through the aorta, and reaches the capillaries through the arteries and arterioles to return to the right atrium through the veins.
- in the pulmonary circulation blood from the right ventricle, and after gas exchange in the lungs ends in the left atrium.
- the coronary circulation starts from the aorta and deals with the blood flow in heart tissue.

The circulation of the blood is achieved through blood vessels, which vary in diameter and thickness depending on the demands of the vascular tree (Figure 1). In general, the diameter of the arteries and the thickness gradually decreases with increasing distance to the heart. In addition, wall properties depend on the position, the stiffness and absorption, which increases proportionally with the distance from the heart in order to maintain an approximately constant blood flow (Silverthorn, 2007).

1.2 Endothelial cell physiology

The lining of every blood vessel is composed of a monolayer of specialized cells called Endothelial Cells (ECs), directly involved in the transport and exchange of molecules and hormones (Bouïs et al, 2001). This monolayer termed endothelium is surrounded by a layer of smooth muscle cells and pericytes (Figure 1). ECs have multiple functions: exchange, metabolic, hemostatic and vascular tone regulation ought to be highlighted.

Endothelium functions as a permeable selective barrier allowing transcellular passage of water, respiratory gases, small molecules and even certain macromolecules; and para-cellular transmigration of leukocytes (Renkin and Curry, 1982). Tight and adhering junctions compose the intercellular connection system, which have a strong anchor to the cytoskeleton. VE-cadherin is the most relevant adhering junction, whose phosphorylation directly influences vascular permeability, angiogenesis and leukocyte transmigration (Chiu et al., 2004).

ECs synthesize and release vasodilators: nitric oxide (NO), prostacyclin and adenosine, which are counteracted in a constant balance with other vasoconstrictor such as endothelin-1, angiotensin 2 and thromboxane A2. NO is derived from L-arginine by the action of nitric oxide synthase (NOS), which can have multiple isoforms. Endothelial NOS (eNOS) is calcium-calmodulin-dependent and has a constitutive expression. It generates small amounts of NO for short periods and its activity is regulated by vasoactive agents such as acetylcholine and bradykinin (Nathan and Xie, 1994).

NO has also other vital biological functions such as non-adherent platelet effect, inhibits adhesion of leukocytes to the vascular wall, reduces the proliferation and migration of smooth muscle cells and inhibits apoptosis in ECs by inhibiting the activation of the caspase 3 (Dimmeler et al., 1999).

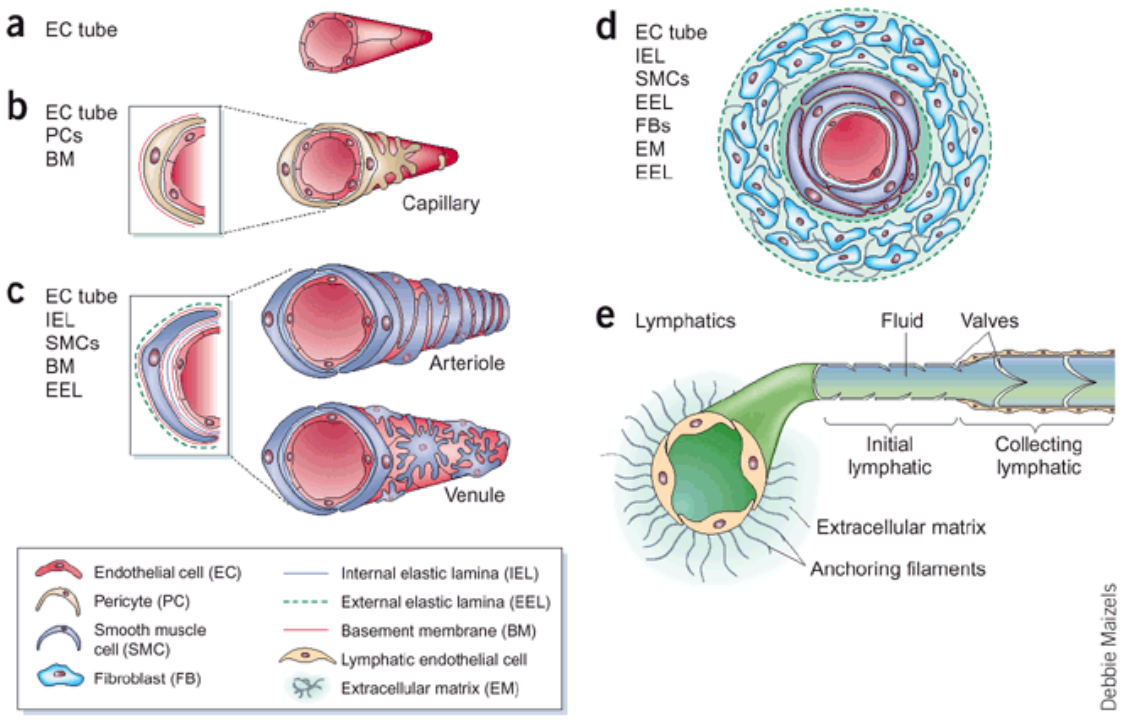

Figure 1 Wall composition of forming vessels. (a) A forming vessel consists of an EC tube. (b) Capillaries are composed of EC tube surrounded by pericytes embedded in the EC basement membrane. (c) Arterioles and venules are surronded by a layer of smooth muscle cells forming an internal elastic lamina. (d) Larger vessels have a thicker wall composed of three layers: Intima composed of ECs, Media composed of smooth muscle cells and matrix and elastic laminae; and Adventitial layer which has its own blood supply. (e) Lymphatic vessels, which collect excess fluid, lack a layer of pericytes. They are composed of valves that pump the flow in one direction. The anchoring filaments allow the vessel to connect to the extracellular matrix. (Jain, 2003).

1.2.1 Shear stress

All blood vessels are endowed bodies of a single layer of ECs and play a key role in the detection of chemical and mechanical environment of the vessels. This mechanical stimulus acting on ECs is called shear stress, for which ECs have shear sensors. The inner layer of blood vessels is constantly exposed to shear stress created by the blood flow. It is defined as the drag force per unit area acting on ECs caused by the local velocity gradient. It is calculated as the product of shear rate and viscosity. Changes in shear stress are translated by the endothelium through a complex signaling network which includes the first ion channels and cellular glycocalyx point. Subsequently, it can modify gene expression in these ECs. There is a relationship between the detection of shear stress, production of free

radicals and the functional and structural adaptation of the blood vessels. Laurindo et al. (1994) demonstrated free radical formation after changes in flow both *in vitro* and *in vivo*, since then, it has been established that shear stress causes not only the generation of NO but also free radicals in ECs and in other tissues.

The average physiological shear stress values are between 0.1 and 0.6 Pa in the veins and between 1 to 1.5 Pa in the arteries (Mongrain and Rodés-Cabau, 2006). It is estimated from the ratio of Poiseuille and it is useful for understanding vascular adaptation, if shear stress increases proportionally to the flow. Detection and signaling of these changes induce an increase in the radius of the vessel by expansion and remodeling, restoring the shear stress to its original level. Therefore, shear stress is fundamental to regulate vessel size and blood flow. Impaired blood flow in large vessels lead to pathological vascular remodeling, such as the formation of aneurysms and atherosclerosis, through the involvement of reactive oxygen species and inflammation (Matlung et al., 2009).

The effects of flow disturbance on atherogenesis are generally studied using primary ECs. Although these studies of isolated cells have provided much information about shear stress induced by reactive oxygen species signaling, there are other factors that influence responses in the extracellular matrix. A reason for the different cellular responses to a constant or oscillating linear flow could be the association with specific sensors of effort for each of the flow patterns. There are several arguments that support them. The first one are the potassium channels of the ECs which translate a different signal in regard of the type of flow. Changes in membrane potential produce changes in intracellular calcium levels and activation or inhibition of different enzymes such as eNOS or NADPH oxidase. Other flow sensors are the cytoskeleton, the glycocalyx and cilia. In response to the laminar flow, cells are capable of elongate in the direction of flow, whereas if the flow is oscillatory, cells remain polygonal and static in cell cultures, thus varying their cytoskeletal rearrangements. The glycocalyx is at the luminal side of ECs and acts as a mechano-receptor in such a way that the depletion of glycoproteins can block production of NO. Moreover, some components thereof react with reactive oxygen species and alter its composition (Pahakis et al. 2007).

The current study focuses on the effect of shear stress on gene expression and uses a similar study published by Uzarski et al. (2013) as a reference. The aim of that study was to prove that temporal changes in shear stress patterns would influence the EC expression. They focused on the up and downregulation of gene transcription under a variable range of physiological shear stress conditions, determined by measuring the shear stress in humans *in vivo*. The pulse rate of a healthy male subject was recorded for 12 hours and the data was used to calculate the shear stress magnitude. Based on that data, they designed an *in vitro* model of physiological flow that would stimulate HUVECs in a variable range of shear stress. Cells were seeded on a glass cover slip and affixed to a

parallel plate flow chamber. Gene expression of genes related to inflammation, coagulation, fibrinolysis and eNOS were measured by qPCR. In addition, they measured the amount of nitrate released into the medium. Data shown in Figure 2 will be used to validate the system used in the current project.

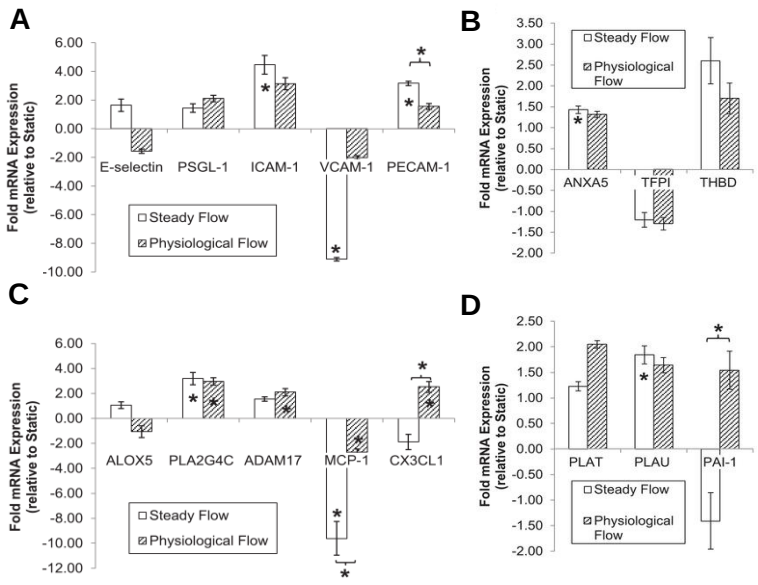

Figure 2 Gene expression measurements under shear stress. Shown is the fold mRNA expression of genes related to (a) homeostasis, (b) adhesion molecules, (c) fibrinolysis and (d) recruitment of inflammatory cells. Modified from Uzarski et al. (2013).

1.3 Inflammatory response in the vessels

Another major role of ECs is modulating the immune system through inflammatory responses of neutrophils, leukocytes, lymphocytes and monocyte mobilization to tissue (Sumpio et al, 2002). For instance, activated lymphocytes expressing integrins like Leukocyte Function-associated Antigen-1 (LFA-1) or Very Late Antigen-4 (VLA-4) interact with ECs through L-selectin receptor, intermolecular cell adhesion molecules 1 or 2 (ICAM-1.2), and vascular cell adhesion molecule (VCAM) (Figure 3) (Huo et al., 2000).

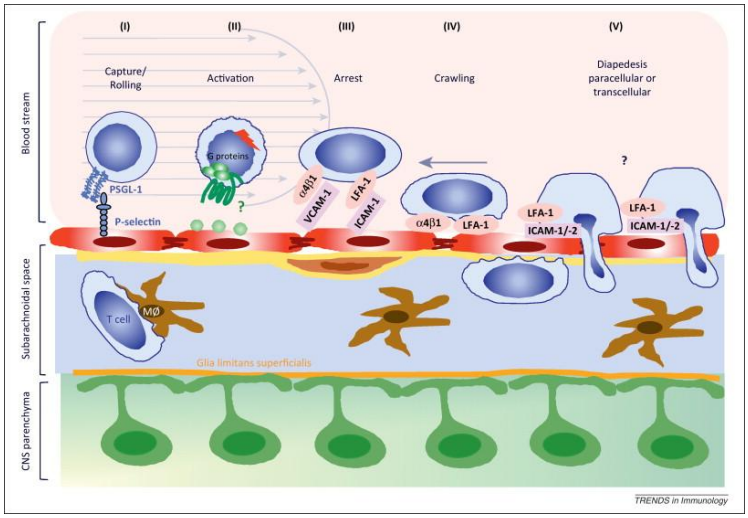

Figure 3 T cell migration across the endothelial barrier. (I) Recognition of antigen on macrophages by T cells triggers inflammatory events leading to the upregulation of adhesion molecules on endothelial cells. P-selectin is then transported to the membrane to attract T cells. (II) Unknown chemokines activate G-protein-dependent integrins. (III) Adhesion molecules such as LFA-1, ICAM-1 and VCAM-1 connect the immune cell to the ECs. (IV) T cell crawls in random directions on the surface of Ecs. (V) The T cell then breaks the endothelial barrier and crosses to the site of infection (Engelhardt and Ransohoff, 2012).

LFA-1 and macrophage 1 antigen (Mac 1) on traversing leukocytes transiently adhere to activated ECs. Moreover, ECs secrete platelet activating factor (PAF), expressing P-selectin and E-selectin while response to cytokine and lipopolysaccharide (LPS) (Luscinskas, 1994). These activated ECs, synthesize interleukin 8 (IL-8) which subsequently stimulates neutrophil chemotaxis and promotes extravasation (to cross the EC barrier from the blood into the tissue).

Another important chemokine is monocyte chemotactic protein 3, coded by the gene CCL7, which is a substrate of matrix metalloproteinase 2, an enzyme which degrades components of the extracellular matrix. The main function of this chemokine is to attract macrophages, monocytes and eosinophils during inflammation and metastasis. Mutations in the CCL7 gene result in a condition known as acute contagious conjunctivitis (Dahinden, 1994), which is the inflammation of the lining of the eyelid and eyeball (The American Heritage medical dictionary, 2007).

An increasing literature suggests that pro-inflammatory microenvironment is closely involved in the development of many chronic diseases such as cancer, diabetes and cardiovascular diseases (CVD) (Tousoulis. D, 2005). Thus, the discordant stimulations of ECs can be hallmark of pathologic states (Shashkin et al, 2005).

1.4 Diseases of the vascular system

CVD are a group of disorders affecting the heart and vascular system, including aneurysms, atherosclerosis, stroke and myocardial infarction among others (WHO, 2016). There are several risk factors that predispose to the development of these conditions. Such factors include: age, gender, hypertension, hyperlipidemia, diabetes, smoking, obesity, sedentary lifestyle, high fat diet, socioeconomic and psychosocial stress and family history of premature CVD (Allender et al. 2008). CVD also include bleeding disorders such as hemophilia, Marfan Syndrome and Hereditary Hemorrhagic Telangiectasia (HHT), which are of genetic origin.

Worldwide, 17.5 million annual deaths are attributed to CVDs, representing 30% of all deaths in the world, 7.3 million of these deaths were due to coronary cardiopathies and 6.2 million to strokes. More specifically, in high-income countries, heart disease and stroke are the first and second leading cause of death (WHO, 2016). In Europe alone, in 2008, CVDs were attributed more than 4.3 million deaths, representing 48% of total recorded deaths on the continent (Allender et al. 2008).

1.4.1 Atherosclerosis and plaque formation

Atherosclerosis is a disease of the intimal layer of the arteries characterized by the proliferation of smooth muscle cells and deposition of lipid, lowering the vascular lumen and forming a plaque (Stary et al., 1994).

Plaque formation has five distinct phases represented in Figure 4 (Fuster et al., 1998):

1. High LDL levels produce an accumulation of LDL in the arterial intima due to an acceleration of plasma exchange. This blood layer will be more prone to oxidation by the presence of free radicals and by the absence of plasma soluble antioxidants (Fuster et al., 1998).

2. LDLs produce polyunsaturated fatty acids and lipoproteins react with lysines and apoprotein B100 oxysterols, which are toxic for ECs (Berliner and Heinecke, 1996).

3. The vascular endothelium and cells exceed their cholesterol storage capacity, leading to the release of pro-atherogenic factors (Sata and Walsh, 1998).

4. The inflammation due to oxidation of LDL is an important factor in the formation of atherosclerotic plaque factor. This oxidative process is based on:

· Inflammatory reaction mediated by T lymphocytes which recognized as foreign to LDL due to the formation of new epitopes.

· Involved in monocyte differentiation to macrophage (Rajavashisth et al., 1998).

· The production of cytokines and glycoproteins cell surface endothelium increases (Khan et al., 1995), making the LDL highly oxidized and making it susceptible to bind to unregulated cellular receptors saturating cholesterol in cells. This process will lead to the formation of foam cells.

5. The formation of potentially atherogenic foam cells is the result of an autoimmune response triggered by these lipoproteins modified by oxidative process. Cells that rapidly become foam cells are macrophages because they recognize oxidized LDL more easily than the rest (Lopes-Virella and Virella, 1996).

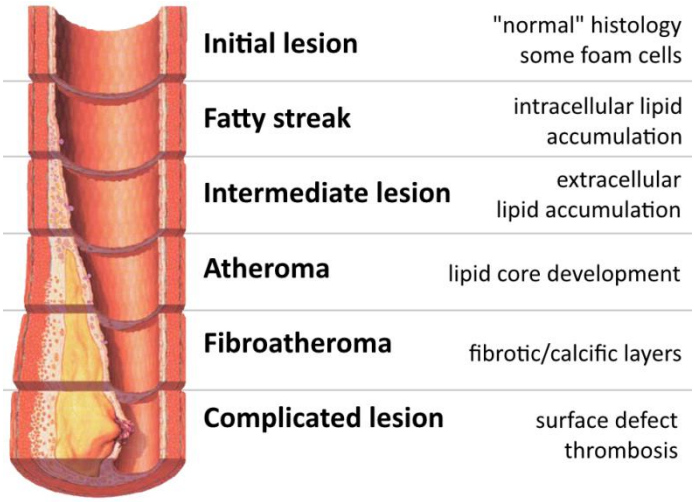

Figure 4 Plaque formation in atherosclerosis (Ucd.ie, 2016).

In 2007, three independent genome-wide association studies (GWASs) reported a locus on chromosome 9p21.3 to be associated with coronary artery diseases (McPherson et al., 2007) (Helgadottir et al., 2007) (Samani et al., 2007). Subsequent studies revealed that the 9p21.3 locus is also linked with abdominal and intracranial aneurysms (Helgadottir et al., 2008) (McPherson, 2010), which are vascular degenerative changes; although the first can occur in association with atherosclerotic plaques, the second is not associated with atherosclerosis. The 59 chromosome 9p21.3 CAD-associated single nucleotide polymorphisms (SNPs) are located in a 58kb linkage disequilibrium block that does not contain any known protein coding genes (Visel et al., 2010) and are 100kb distant from a

cluster of cell-cycle regulating genes (CDKN2A and CDKN2B) encoding the two cyclin-dependent kinase inhibitors p16 and p15. A study focusing on melanoma neural tumor described a new long non-coding RNA (lncRNA) in the 9p21.3 locus, named ANRIL for “antisense noncoding RNA in the Ink4 locus” (Pasmant et al., 2007). Interestingly all CAD-associated genomic variants reported so far are located within ANRIL sequence. lncRNAs differ from protein-coding mRNAs in that they generally reside exclusively in the nucleus and have complex secondary structures, making them difficult to target by conventional RNA interference. In addition and because they have no open reading frames or predicted functionally important domains and are often transcribed from multiple promoters, they are generally hard to target by conventional knockout techniques. In 2011, Gutschner and colleagues reported the efficient silencing of the lncRNA MALAT1 using zinc finger nucleases (ZNF)-mediated genome editing and RNA destabilizing elements. The Cowan lab successfully created CRISPR/Cas9 knock out mutants for ANRIL by inserting a polyA sequence at the end of exon 1 by homologous recombination based on this paper.

1.4.2 Insulin resistance and Diabetes

To understand what Diabetes is, we have to first take a look at the human major source of energy: Glucose. Cells uptake glucose upon binding of insulin by specific receptors (Chang et al., 2004). After a meal (high glucose concentration in blood), insulin is secreted to induce glucose uptake in target tissues, so that the sugar is removed from circulation and converted into storage products such as glycogen. On the other hand, in fasting conditions, glucagon is secreted to trigger glycogen lysis and glucose release (Chang et al., 2004).

Problems arise when the body is unable to produce or detect insulin for the cells to consume glucose, a condition known as diabetes. There are two different types of diabetes, depending on what process related to insulin is impaired. Type 1 Diabetes Mellitus (T1DM) is an autoimmune disease in which the cells that produce insulin in the pancreas (β-cells) are destroyed by the immune system of the patient, which requires daily injections of insulin after every meal. On the other hand, Type 2 Diabetes Mellitus (T2DM) is due to a loss of sensitivity from the cells towards insulin (Alberti and Zimmet, 1998).

The two types of diabetes mellitus known are risk factors for developing ischemic cardiopathies. CVD is two to five times more frequent and has a worse prognosis in patients with diabetes than without it (Melidonis et al., 1999). The risk of myocardial infarction for patients with type II diabetes is as high as coronary patients with myocardial infarction (Haffner et al., 1998). Diabetes mellitus is preceded by a long asymptomatic hyperglycemia. In individuals with impaired glucose tolerance it has also shown an increased risk to develop macrovascular disease (Melidonis et al., 1999).

Diabetes is a concerning problem in the 21st century due to the increased number of people suffering of this disease which is one of the leading causes of death in USA and worldwide (WHO, 2016). The number of people diagnosed with diabetes has risen from 108 million to 422 million in the last 24 years due to the increase in obesity in the world's population (Kahn et al., 2014).

Insulin Resistance and Endothelial Cells

Due to the importance of ECs in insulin transport, EC dysfunctions are closely related to high concentrations of insulin in the blood leading to hyperinsulinemia. Insulin resistance is a condition in which the insulin-induced transport of glucose is decreased in metabolic organs such as adipocytes and skeletal muscle, leading to an increase in hepatic glucose production and impaired lipid metabolism in adipose tissue and liver (Sesti, 2006; Bhattacharya, Dey and Roy, 2007). Patients with insulin resistance are predisposed to developing T2DM. (LeRoith *et al.* 2003).

A way to model hyperinsulinemia in ECs is the constitutive expression of AKT2. A missense mutation pGlu17Lys (E17K) in the AKT2 gene was found in three patients suffering from hypoglycemia, hypoinsulinimia and uneven increased body fat (Hussain et al., 2011). This mutation was found to constitutively activate the insulin pathway (Figure 5) (Ding et al. 2013; Hussain et al., 2011). To study the functions of the constitutively active Akt2, our laboratory designed hPSCs clones carrying AKT2 E17K mutation (Ding et al. 2013). When cells are differentiated into adipocytes, they show higher IL-8 (an inflammatory adipokine) expression, and an increased glucose uptake and triglyceride count (Ding et al. 2013). The Cowan lab successfully created knock out mutants for AKT2.

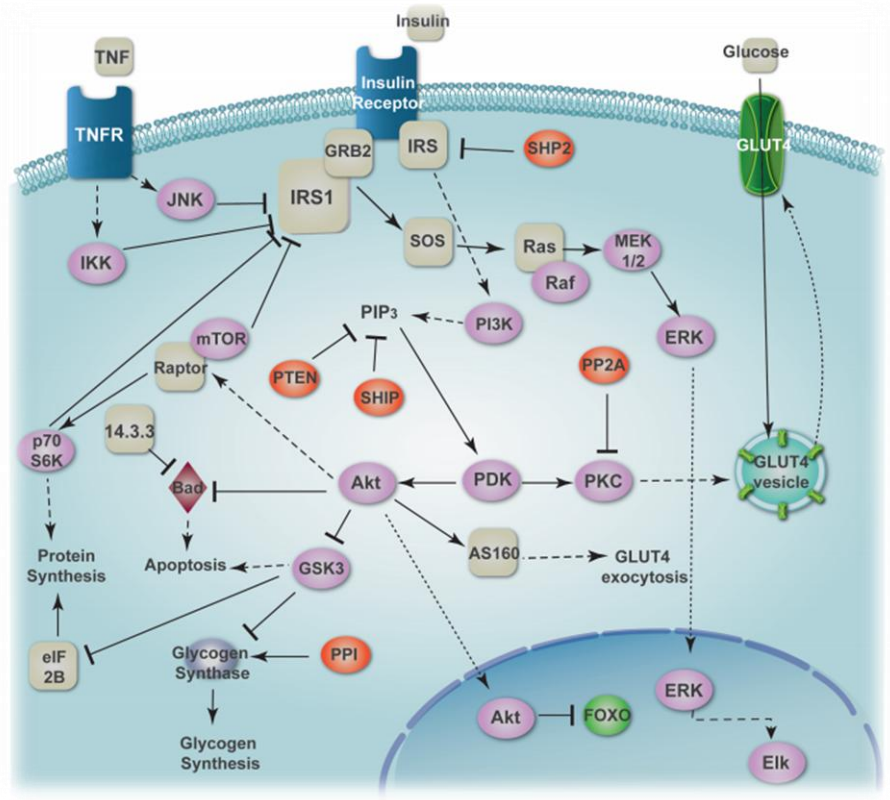

Figure 5 Canonical insulin signaling pathway. (Tocris Bioscience, 2016)

1.4.3 Marfan Syndrome

Marfan syndrome, one of the most common of the so-called "rare diseases", is a genetic disorder of the connective tissue with pleiotropic manifestations involving the heart, blood vessels, lungs, eyes, bones, ligaments, skin and the dura mater covering the Central Nervous System (Pyeritz, 2000). It can be inherited as an autosomal dominant trait and its incidence is one per 5,000-10,000 people. It affects all ethnic groups and genders equally. However, 15 to 30% of cases have no family history and are called "sporadic", meaning that they are caused by a *de novo* mutation (Robinson et al., 2002).

This disease causes skeletal defects that are generally recognized due to the patient's long limbs, spider fingers, thoracic malformations, column curvature and a particular set of facial features including malocclusion teeth and a curved palate. Survival is mainly determined by the severity of cardiovascular malformations, with aortic pathology (rupture or aortic dissection) and heart failure caused by mitral or aortic regurgitation, the most frequent causes of death. About 90% of patients with Marfan syndrome will have a cardiovascular complication during their lifetime, including surgery of the aortic root, aortic dissection or mitral valve surgery (Robinson, 2000).

The connective tissue function is to support and assist in the growth of cells that constitute the body. The complication in Marfan's syndrome type I lies mainly in fibrillin, an essential elastin protein that forms elastic fibers of connective tissue, giving strength and malleability to the tissue (Robinson, 2000). A mutation in the transforming growth factor β receptor type II (TGFBRII) causes Marfan syndrome type II, which is associated with Loeys-Dietz aneurysm syndrome. TGFBRII is a transmembrane protein with cysteine-rich extracellular region and an intracellular region containing a serine/threonine binding domain (Figure 6) (Singh et al., 2006). The Cowan lab successfully created knock out mutants for Marfan syndrome type II by removing exon 1 using CRISPR/Cas9 technology.

1.4.4 Hereditary Hemorrhagic Telangiectasia

Hereditary Hemorrhagic Telangiectasia (HHT), also known as Rendu-Osler-Weber syndrome, is also one of the most common of the so-called "rare diseases", characterized by the presence of weak vessel walls leading to the appearance of arteriovenous malformations (Braverman, Keh and Jacobson, 1990). Such malformations can occur in skin and mucosa resulting in the appearance of telangiectasia, and those present in the nasal mucosa lead to epistaxis (recurrent nosebleeds) (Berg, 2003). Larger arteriovenous malformations can occur in internal organs such as lung, liver and brain and its evolution can trigger internal bleeding that could have fatal consequences for the patient if not treated early.

There are 5 types of HHT based on the gene or locus affected. In over 90% of cases the mutations are located in ENG (Endoglin gene) or ACVRL1 (ALK-1 gene), leading to HHT1 and HHT2 respectively. In 10% of the remaining cases the mutation can be located on a locus of chromosome 5 (unidentified gene), a locus on chromosome 7 (unidentified gene) or in GDF2 (BMP9 gene). Finally, it has been identified a syndrome known as Juvenial polyposis associated with HHT caused by mutations in MADH4 (Smad4 gene). All identified genes encode proteins implicated in the TGF-β pathway (Whitehead, Smith and Li, 2012). The Cowan lab successfully created knock out mutants for HHT by removing exon 1 using CRISPR/Cas9 technology.

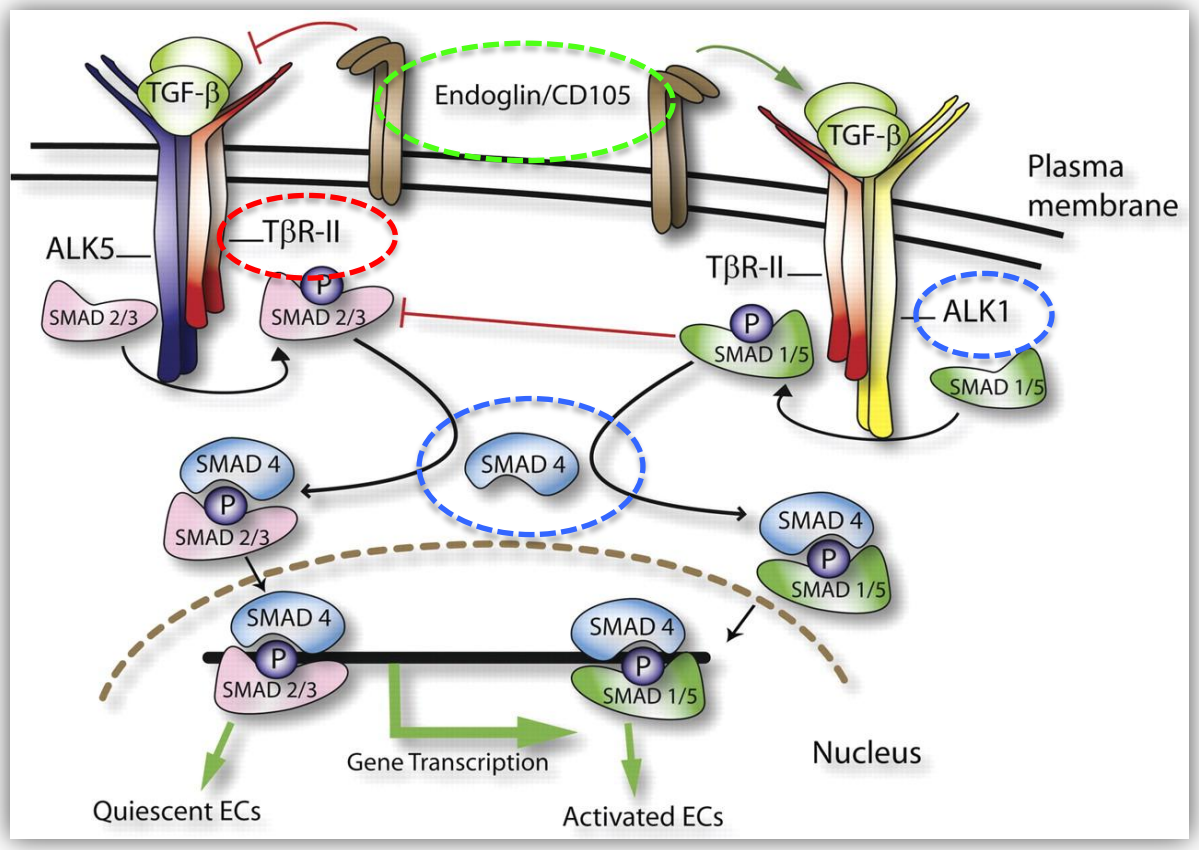

Figure 6 TGF-β pathway. Mutations in this pathway cause Marfan syndrome and HHT. Endoglin (marked in green) involved in HHT2, TβR-II (marked in red) involved in Marfan syndrome type II, SMAD 4 and ALK1 (marked in blue) involved in HHT1.

1.5 Genome Engineering techniques

Genome editing is an extremely powerful tool to introduce, modify or delete genes. Nucleases are one of the tools generated to solve the problem of random gene insertion and allow specific modification of the genome. They were designed to introduce specific forms a double-strand break (DSB) at a particular DNA site, that after being repaired by homologous recombination (HR) or non-homologous end joining (NHEJ), allows targeted modifications in the genome (Jensen et al., 2011). Depending on the mechanism used for the repair of DSBs, different genetic modifications are obtained. Thus, by the NHEJ mechanism, chromosomal fragments may be deleted sometimes resulting in the disruption of expression of a gene (knock-out). On the other hand, the HR mechanism allows for a gene insertion into a homologous (knock-in) or heterologous (gene addition) region.

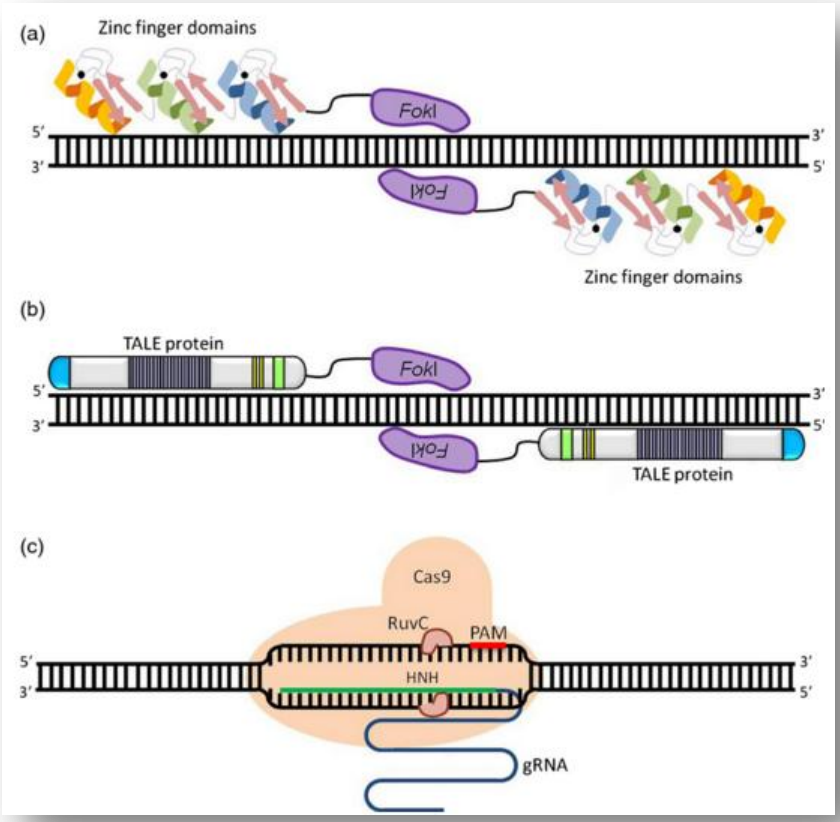

Figure 7 Schematic representation of the three common engineering tools. (a) ZFNs: composed of DNA recognition domains and *FokI* nuclease catalytic domain fusion. (b) TALENs: composed of TALE central DNA binding domain and *FokI* catalytic domain fusions. (c) CRISPR/Cas9: composed of Cas9 protein which includes guide RNA (gRNA) that recognizes a specific Protospacer Associated Motif (PAM) sequence.

The three major techniques of genome editing will briefly be described here in chronological order they were developed: Zinc finger nucleases (ZFNs), transcription activator-like effector nucleases (TALENs) and clustered regularly interspaced short palindromic repeats (CRISPR) and CRISPR associated protein 9 (Cas9) (Figure 7). All three exploit properties to repair DNA once a DSB is induced (Gaj et al. 2013).

1.5.1 ZNFs

ZNFs are artificial DNA nucleases that are constructed by merging several ZF domains with the nuclease domain of restriction enzyme *FokI* type IIS (Chandrasegaran and Smith, 1999). Such domains are composed of a set of three to five ZF Cys2His2, have the function of DNA-specific binding and direct ZFN to its target DNA, while the endonuclease domain has a DNA cutting enzymatic activity.

The ZF Cys2-His2 domain is the DNA most common binding motif in the human proteome and consists of 30 amino acids in ββα configuration, where the α helix joins the DNA major groove and recognizes three to four bases adjacent nucleotides (Pabo, et al., 2001). The modular structure of the ZF motif allows the development of several series of domains, enabling the recognition of almost any target in the genome of any species.

It is known that the domain *FokI* (from prokaryotic Flavobacterium okeanokoites) cuts DNA nonspecifically as a dimer and that this cut occurs more efficiently when the dimer is in reverse orientation (Smith, 2000). The optimum configuration for ZFN design is as heterodimers that recognize a DNA sequence of 18-24 bp with space of 4-6 bp between binding sites (Bibikova et al., 2001). Each monomer ZFN comprises three or four ZF domains that recognize a target DNA sequence of 9 to 12 bp, and, in turn, each typical domain ZF contains an α-helix that specifically recognizes a triplet of DNA. Once the DSB has been generated by ZFNs, the cell may primarily activate two different mechanisms to repair the damage, HR, which is the preferred route when high amounts of donor DNA are available, and on the other path NHEJ (Cathomen and Keith Joung, 2008).

1.5.2 TALENs

The TALE proteins were identified in a gram-negative γ-proteobacteria from the genus Xanthomonas. Bacteria belonging to this genus are pathogens of plants and secrete a mixture of effector proteins that they introduce into host cells; these proteins function as transcription factors in eukaryotes. Among the set of secreted proteins are those of the TALE family. TALEs are introduced directly such in the cell cytoplasm and transported to the nucleus. By recognizing specific promoters and interacting with the basal transcription machinery, transcription of specific genes of the host plant is induced (Jankele and Svoboda, 2014).

TALEs recognize the DNA sequences of the host cells through the tandem repeats of the central domain, which consist of 1.5-33.5 repeated sequences. Each of these repeats comprises between 33 and 35 highly conserved amino acids, except those located in positions 12 and 13. Repeat variable di-residues (RVDs) are found in these positions, which confer specificity for the corresponding nucleotide of the target sequence (Deng et al., 2012).

Due to the properties of these effectors, TALE nucleases (TALENs) have been developed from them, a useful tool in the field of genetic engineering. The construction of the TALEN is based on the association of DNA specific binding domain of TALE to the catalytic domain of the FokI endonuclease. As the catalytic domain functions as a dimer, it is

necessary to generate two structures with a specific binding domain to nucleotide sequences of each of the DNA strands, positioned in opposite orientation (Deng et al., 2012).

The construction of the TALEN is based on sequential ligation of several fragments (between 15 and 18 generally). Said fragments present a particular orientation that is given by a specific sequence, allowing ligation of the fragments in an oriented manner. A plasmid (called backbone) is used to construct it, which has a resistance gene to an antibiotic (kanamycin or ampicillin). Once the complete sequence is acquired, the construction of the nuclease ends with a fusion within a single plasmid of the coding sequence for the *FokI* nuclease (Deng et al., 2012).

1.5.3 CRISPR/Cas9

CRISPR/Cas9 was initially described as a mechanism of the adaptive immune system that prokaryotes used to prevent viral infections (Bhaya, Davison and Barrangou, 2011). A few years later, this mechanism was used to develop the most efficient genome engineering technique so far. CRISPR genome editing techniques are used in several organisms, including humans (Selle and Barrangou, 2015). The first time the CRISPR/Cas9 technology was successfully used in eukaryotic cells was described by Cong et al. in 2013. They engineered two Cas9 orthologues from S. thermophilus and S. pyogenes and used them to cleave human and mouse cells. Moreover, they proved that the system could be programmed to target multiple genomic loci and that it could drive a homology-directed repair (Cong et al. 2013).

This system consists of a protein multi-domain Cas9 having two domains nuclease activity (Makarova et al., 2006). This protein forms a ternary complex with two molecules of RNA: with crRNA (CRISPR RNA) and the tracrRNA (trans-activating RNA CRISPR) that partially complements the crRNA (Deltcheva et al., 2011). The crRNA has 42 nt, of which 22 nt are a repeated sequence and 20 nt form the spacer sequence, which is responsible for guiding the Cas9 protein to the target DNA, while the tracrRNA is necessary for the maturation of crRNA and guiding Cas9 to the cutting position (Karvelis et al., 2013).

The CRISPR/Cas9 consist of a set of several conserved short repeats separated by a unique spacer DNA sequence which originates from a phage or a plasmid DNA. The spacer sequence is then used as a template to generate small RNA molecules which, in combination with Cas proteins, lead to a effector complex that silences foreign nucleic acids. This is because the Cas9 site mediates a DSB cut in the target DNA after joining this sequence. This site, called protospacer, comprises a nucleotide that binds crRNA and a

short nucleotide sequence referred to as Protospacer adjacent motif (PAM). It is necessary that both sequences are present for Cas9 to join the target sequence and generate the link between DNA and crRNA (Jinek et al., 2012).

CRISPR/Cas9 system can be redesigned easily by the modification of crRNA. Therefore, CRISPR/Cas9 has been used as a new tool for genetic editing since it is relatively easy to generate specific DNA sequences encoded by crRNA (Barrangou, 2012).

Some of the advantages of this new technology compared with ZFNs and TALEN are:

- The design of these proteins is achieved by building RNAs, which makes it faster and cheaper compared to the design of other nucleases as ZFN or TALEN (Wang et al., 2013).
- Secondly, there are Cas9 mutants that can introduce cuts in the target, both in the top and bottom chain which opens up new possibilities in DNA repair by HR (Cong et al., 2013).
- Lastly, several mutations can be introduced simultaneously by introducing various RNAs targeting separate genes (Wang et al., 2013).

This system is constantly evolving with new ways to use it, and improvements being published every week. Moreover, enzymes having similar properties as Cas9 are studied as alternatives. For instance, Zetsche et al. (2015) discovered the cpf1 enzyme which only needs one RNA molecule and creates sticky ends when cutting DNA.

1.6 Aim

Human disease modeling enables the understanding of cellular and molecular mechanism of disease to develop more efficient treatments (Avior, Sagi and Benvenisty, 2016). A disease model is a representation of the abnormal animal or human biology that occurs in a particular disease. The model must reproduce aspects of a disease, or even the complete pathology of the disease outside the human body (Pandey and Nichols, 2011).

The use of hPSCs to model human disorders have been enhanced with the emergence of two recent techniques: pluripotent stem cell differentiation and genome engineering. These techniques open the road to new ways of modeling human disorders, especially for syndromes that are not easily reproduced in animal models. For instance, mice do not develop CVD in the wild. Current murine models of CVD require mutations in key regulators of their lipoprotein metabolism and need specific diets (Zaragoza et al., 2011).

Generating mutant hPSCs clones and differentiating them into a cell type of interest has recently become faster and easier. The current challenge is now to design experimental conditions that mimic both wild type and pathogenic state of a given human disorder. For instance hPSCs-derived cells do not always recapitulate the gene expression patterns observed in primary cells or *in vivo*. This could in part be explained by the fact that cells in a body are part of a system in which they adhere on a complex extracellular matrix and constantly receive information (signals transported by the blood, mechanotransduction, interactions with neighboring cells) whereas differentiated cells lie alone on plastic or a very simple extracellular matrix (often fibronectin or collagen).

The current study focuses on vascular disorders and the use of mechanical stimulus to improve gene expression in cell based models. More precisely, the aim of this project is to investigate the gene expression of hPSC-ECs with various knockouts related to the vascular system, in a microfluidic chamber to mimic blood flow to create a more accurate disease model. Understanding the molecular mechanisms involved in the actions of TGF-B bleeding disorders is important for developing new therapeutic tools in the treatment of these diseases. This project can be further divided in three main objectives.

This project objectives are: 1) To design a tool to apply shear stress on ECs, 2) To test and compare gene expression of primary cells, hPSC-ECs and knockout hPSC-ECs in static and physiological conditions, 3) To characterize and validate the functionalities of hPSC-ECs, 4) To successfully knock out CCL7 gene in hPSCs.

By investigating the role of the TGF-β pathway in human ECs using hPSC-ECs, I hope to gain further insight into the complications of diabetes and CVDs.

2 Materials and Methods

2.1 Cell lines

The iPSC line Sev-A 1016 used in this study was a kind donation from the Melton laboratory (HSCRB) (Chetty et al. 2013).

HCAECs and HUVECs were purchased from Lonza and cultured in EMG-2 MV (Lonza).

Human Embryonic Kidney cells (HEK 293T) were purchased from ACCT and cultured in DMEM, supplemented with 10% of heat inactivated FBS (Life Technologies).

2.2 Maintenance of hPSCs

The Sev-A 1016 were cultured on geltrex (Life Technologies) matrix pre-coated dishes (1:30 in DMEM (VWR) for one hour (Schinzel et al., 2011)). The media used for all hPSCs was mTeSR1 (STEMCELL Technologies) supplemented with penicillin/streptomycin (10.000 I.U. Penicillin, 10.000 µg/ml Streptomycin) (corning cellgro) and plasmocin (Invivogen). Media was replaced every 24 hours (15-20 ml). Cells were kept at 37ºC and 5% CO_2 and routinely passaged when they were 85-95% confluent with accutase (STEMCELL Technologies) diluted in a 1:5 ratio in PBS. For each passage, Sev-A 1016 were treated with 10 µM of Rock inhibitor (Y-27632, Santa Cruz Biotechnologies, sc-281642A) to enhance attachment.

2.3 Endothelial cell differentiation from hPSCs

Cells were seeded at a density of 37.000 hPSCs per cm^2, in a T175 flask with a vent cap (Corning). After 24 h, the media was replaced by N2B27 (composed of 1:1 Neurobasal medium (Life technologies) and DMEM/F12 medium (Life technologies) supplemented with Glutamax (Life technologies), B27 (Life technologies), N2 (Life technologies) and β-Mercaptoethanol (Life technologies)), supplemented with 8 µM CHIR-99021 (Cayman Chemical) and 25 ng/ml BMP4 (R&D Systems). Cells were incubated for 4 days with no media change.

On day 4, media was replaced by StemPro-34 SFM (Life Technologies) supplemented with 200 ng/ml VEGF (Peportech) and 2 µM foskolin (Abcam). Media was changed on day 5

and 6. On day 6, CD144 positive ECs were sorted by Magnetic-activated cell sorting (MACS) (Miltenyi Biotec) using magnetic CD144 (VE-Cadherin) microbeads (Miltenyi Biotec). Cells were resuspended in 80 µl of buffer and 20 µl of CD144 MicroBeads per 10^7 cells and incubated for 20-30 minutes at 4ºC. Cells were then dissociated and filtered through a 30 µm nylon mesh to remove clumps. They were washed with buffer and centrifuged at 1000 rpm for 5 minutes. Before proceeding to the magnetic separation, approximately 10^8 cells were resuspended in 500 µl of buffer.

The 1016 Sev-A ECs were cultured on human fibronectin pre-coated plates (2.5 µg/ml) of human fibronectin (VWR) in DPBS (Corning) for 2 hours and kept in Stempro medium supplemented with 50 ng/ml. When confluent, 1016 Sev-A-ECs were dissociated by using 1:10 accutase.

2.4 RNA extraction, Rt PCR and qPCR

RNA extractions were performed using the RNeasy Mini Kit from Qiagen following the manufacturers manual.

The samples were subjected to reverse transcriptase (RT) reaction to synthesize cDNA. cDNA was amplified by qScript™ cDNA synthesis kit (Quanta Bio) in a 20 µl reaction mixture containing 4 µl of SuperMix 5X and 2 µg of template RNA. Rt-PCR profile consisted of 5 min at 94ºC, followed by 30 min at 42ºC and 5 minutes at 85ºC. The samples were stored at 4ºC before further analysis by qPCR.

The qPCR reaction preparation was performed according to the Taqman protocol. The final reaction volume of 10 µl contained 5 µl of Taqman probe (Applied Biosystems), 0.5 µl of probe and 4.5 µl of cDNA template. Thermocycling was performed in a ViiA™ 7 Real-time PCR system (ThermoFisher). qPCR profile consisted of initial denaturation at 95ºC, followed by 40 cycles of a denaturation step of 15 s of at 95ºC and a step of 1 min at 60ºC. The reaction finished by the built in melt curve.

Table 1 qPCR probes

Probe	Gene	Species	Vendor	Catalog Number
Homo sapiens ribosomal protein lateral stalk subunit P0	RPLP0	Human	Thermofisher	4310879E
nitric oxide synthase 3	eNOS	Human	Thermofisher	Hs01574659_m1
vascular endothelial growth factor A	VEGF	Human	Thermofisher	Hs00900055_m1

Endothelin-1	EDN-1	Human	Thermofisher	Hs00174961_m1
superoxide dismutase-1	SOD-1	Human	Thermofisher	Hs00533490_m1
platelet/endothelial cell adhesion molecule 1	PECAM1	Human	Thermofisher	Hs00169777_m1
intercellular adhesion molecule 1	ICAM1	Human	Thermofisher	Hs00164932_m1
vascular cell adhesion molecule 1	VCAM1	Human	Thermofisher	Hs01003372_m1
selectin E	SELE	Human	Thermofisher	Hs00950401_m1
Kruppel-like factor 2	KLF2	Human	Thermofisher	Hs00360439_g1
Annexin 5	ANXA5	Human	Thermofisher	Hs00996187_m1
Urokinase plasminogen activator	PLAU	Human	Thermofisher	Hs01547054_m1
Fractalkine	CX3CL1	Human	Thermofisher	Hs00171086_m1
ADAM metallopeptidase domain 17	ADAM17	Human	Thermofisher	Hs01041915_m1
cytosolic phospholipase A2 gamma	PLA2G4C	Human	Thermofisher	Hs01003743_m1
activin A receptor type II-like 1	ACVRL1	Human	Thermofisher	Hs00953798_m1
Endoglin	ENG	Human	Thermofisher	Hs00923996_m1
V-Akt Murine Thymoma Viral Oncogene Homolog 2	AKT2	Human	Thermofisher	Hs01086102_m1
Cyclin-Dependent Kinase Inhibitor 2A	CDKN2A	Human	Thermofisher	Hs00923894_m1
Cyclin-Dependent Kinase Inhibitor 2B	CDKN2B	Human	Thermofisher	Hs04259476_m1
Krev interaction trapped-1	KRIT1	Human	Thermofisher	Hs01090981_m1

2.5 Immunofluorescence staining

Cells were fixed with 4% PFA (paraformaldehyde) (Sigma-Aldrich) and incubated at room temperature for 15 mins. The wells were rinsed three times with PBST (PBS + 0.1% Triton X). Kept in blocking buffer composed of PBST+BSA 5% for one hour on an agitating plate. Primary antibody (concentration shown in table 1) mixed with blocking buffer was added and incubated at 4ºC overnight. The next day, cells were washed three times with PBST for 10 minutes on an agitating plate. Secondary antibody was added (concentration shown in table 2) and incubated for one hour avoiding light. Finally, the plate was washed 3 times before application of DAPI. Images were acquired using an inverted microscope (Axiovert 200).

Table 2 Primary Antibodies

Antigen	Host	Dilution	Vendor	Catalog Number
VE-Cadherin	Goat	1/100	R&D Systems	AF938
vWF	Rabbit	1/400	Dako	A0082
PECAM1	Sheep	1/100	R&D Systems	AF806

Table 3. Secondary Antibodies

Antigen	Host	Dilution	Vendor	Catalog Number
anti-sheep IgG Alexa Fluor 569	Donkey	1/1000	Invitrogen	A21099
anti-goat IgG Alexa Fluor 546	Donkey	1/1000	Lifetechnologies	A11056
anti-mouse IgG Alexa Fluor 555	Donkey	1/1000	Lifetechnologies	A31570

2.6 Angiogenesis assay

400 µL of cold Geltrex Matrix (Life Technologies) was carefully added to each well of a 24 well plate. The plate was incubated for 30 minutes at 37˚C to solidify the matrix. ECs were resuspended in Medium 200 (Invitrogen) with LSGS (Invitrogen) at a cell density of $1x10^6$ cells/ml. 300-500 µL of cell suspension was added to each well. The plate was incubated at 37˚C overnight. The next day, images were acquired using an inverted microscope (Axiovert 200).

2.7 CRISPR/Cas9

The current protocol was set up in the Cowan laboratory. A detailed version written by Dr. Peters et al. (2013) can be found at stembook.org.

2.7.1 CRISPR and primer design

The human genomic sequence of the target exon was identified through NCBI database and the 20-mer single guide RNA (sgRNA) and 3-mer sequence of Protospacer Adjacent Motif (PAM) at recognition site were designed using MIT CRISPR design tool (crispr.mit.edu). The off target score was estimated through the same tool. In order to construct plasmid containing markers for selection, “CACC” before the 20-mer guide

sequence (5'-CACCG-19) and "AAAC" before the guide's reverse complement (C-19-CAAA-5) were added. APE software was used to edit and visualize CRIPSR and primers. Primers were designed in NCBI primer blast to target exon 2 and exon 3.

Table 4 CRISPR and primer sequences

Forward Primers	CTGAGACCAAACCAGAAACCTC
	CTCCTTCTCCTTGAAGCACATT
	AGAAAAAGGATAAGGGGTGAGC
Reverse primers	TGGGCAGGGAATAGGACTAGTA
	TGAACTGAAAACAAGCCATGAC
CRIPSRs	CACCCTCCAACATGAAAGCCTCT 5'-CACCGACCCTCCAACATGAAAGCC-3' 5'AAACGGCTTTCATGTTGGAGGGTC-3'
	GGGGCTTGCTCAGCCAGGTAAGG 5'-CACCGGGGCTTGCTCAGCCAGGTA-3' 5'AAACTACCTGGCTGAGCAAGCCCC-3'
	GCAGCTGCTTTCAGCCCCCAGGG 5'-CACCGCAGCTGCTTTCAGCCCCCA-3' 5'AAACTGGGGGCTGAAAGCAGCTGC-3'
	GAAAATCCCTAAGCAGAGGCTGG 5'-CACCGAAAATCCCTAAGCAGAGGC-3' 5'AAACGCCTCTGCTTAGGGATTTTC-3'
	CACAGAAGTGGGTCCAGGACTTT 5'-CACCGACAGAAGTGGGTCCAGGAC-3' 5'AAACGTCCTGGACCCACTTCTGTC-3'

2.7.2 Primer validation

Primers were validated by running a PCR with genomic DNA of hPSCs. The components of the PCR included 4 µl of 5X Phusion HF buffer, 1.6 µl of dNTPs, 0.1 µl of forward and reverse primers, 0.1 µl Phusion DNA polymerase, 1 µl DNA and water added up to a total volume of 20 µl. PCR profile started by 5 min at 94ºC, followed by 34 cycles of 30 seconds at 94ºC, 30 seconds in a gradient of 50-70ºC and 1 minute at 72ºC. The last step consisted of 10 minutes at 72 ºC. The samples were then analyzed in a 1.5% agarose gel.

2.7.3 Annealing, phosphorylation, ligation and transformation

Oligos were annealed by making a mixture of 2 µl of sense, 2 µl of antisense, 20 µl of 10x Annealing Buffer and 176 µl of water. The mixture was heated at 95ºC for 2 minutes in a PCR machine and allowed to cool down at room temperature.

To proceed with the phosphorylation, 4.8 µl were taken from the mixture above and mixed with 0.6 µl enzyme T4 PNK and 0.6 µl buffer T4 PNK. This time, the mixture was kept at 37ºC for 30 minutes and at 50 ºC for 20 minutes.

As the last step, ligation, 6 µl of the phosphorylated oligo was taken and mixed with 1 µl of vector pCGT, 1 µl of 10 ligase buffer, 1 µl of T4 ligase and 1 µl of distilled water. The mixture was incubated at room temperature for one hour.

For transformation, the ligated oligos were added to 50 µl of E. coli and they were exposed to heat shock treatment. This treatment consisted of keeping the mix in ice for 5 minutes, placing it in a water bath at 42ºC for a minute and a half and placing it back in ice for 2 minutes. Then, the transformed bacteria were plated in a plate containing ampicillin.

2.7.4 Miniprep

The next day, colonies were picked and placed in a tube containing LB broth, in which they were grown overnight at 37ºC in a shaker at 220 rpm and the next day, bacteria were spinned down at 4000 rpm for 10 minutes. The supernatant was discarded and the cells were resuspended in 300 µl of PBS. 50 µl of 7x lysis buffer (containing 5% SDS (12.5ml 20%), 0.8N NaOH (4ml 10N), 5mM EDTA (0.5ml 0.5M), 7% Isopropyl Alcohol (3.5ml) and pinch of bromothymol blue) was added and mixed until the solution turned transparent and viscous. Then, 200 µl of neutralizing buffer (containing 0.6M KOAc (5.8g), 0.3M Malic Acid (4g), 2.5M GuHCl (23.8g) and a pinch of phenol red) was added and mixed. Tubes were centrifuged at high speed for 5 minutes and transferred into a spin minicolumn (Epoch Life Science). Tubes were centrifuged at 14000 rpm for 30 seconds. 200 µl of endo wash (containing 5M GuHCl (47.6g) and 30% Isopropyl Alcohol (30ml)) was added and centrifuged for 30 seconds. The supernatant was discarded and 700 µl of wash buffer (containing 10mM Tris pH 7 (1ml of 1M stock) and 80% EtOH (80ml of 95%)) was added. Tubes were centrifuged for an additional minute. The column was placed in a new tube and DNA was eluted with 50 µl of elution buffer (containing 10mM Tris pH 8.0 (0.5ml of 1M stock)) and centrifuged for a minute. Samples were sent to genewiz for sequencing.

2.7.5 Transfection into 293T cells

HEK 293T cells were transfected by using FuGENE® HD Transfection Reagent. The protocol provided was followed and is briefly described below. Cells were plated in a 6-well plate at a density of 80%. The next day, a mixture of 3102 µl of media containing 66 µg of DNA and 198 µl of FuGENE® HD reagent was prepared and vortexed briefly. 150 µl was added to each well. gDNA was then extracted using DNeasy® Blood and tissue kit (Qiagen). The manufacturers protocol was followed. DNA was amplified by PCR and an electrophoretic gel was run.

2.7.6 hPSC Electroporation

1.5 x 10^6 Sev-A 1016 cells were resuspended in 800 µl of ice cold PBS containing 25 µg of pCas9_GFP plasmid and 25 µg of gRNA expression plasmid and transferred to a 0.4 cm electroporation cuvette (BioRad) and incubated for 5 minutes on ice. Electroporation was performed with Gene Pulser XCell™ (BioRad), with 250 V and 500 µF as parameters. Cells were quickly transferred into fresh media, centrifuged at 1000 rpm for 5 minutes and plated on a pre-coated plate.

2.7.7 FACS

After 48 hours following electroporation, efficiency was assessed by GFP visualization under microscope (Axiovert 200). Cells were detached with accutase to ensure single cell dissociation. The cells were resuspended in 500 µl of PBS with 10 µM Rock inhibitor and passed through a 35 µm cell strainer into a FACS tube (VWR). Cells were then sorted by BD FACSAria™ II flow cytometer and the GFP positive cells were collected into an Eppendorf tube containing 700 µl media with 10 µM Rock inhibitor. Cells were then seeded in condition media into a Geltrex 10 cm coated dish at a density of 15,000 cells per 10 cm dish. The media used is conditioned which means that it contains half recycled mTeSR1 and half fresh mTeSR1.

2.7.8 Picking colonies

Colonies were closely monitored and picked when they were about the size of a nickel (usually 10-12 cm). The media was replaced by PBS. The colonies were picked with a pipette and placed in individual wells in a 96-well plate. Media was changed every 24 h

until cells reached a confluency of 80%. Cells were split into three 96-well plates of which, one was used for gDNA extraction.

2.7.9 Screening

gDNA was isolated by using PREPGEM (Zygem 95044-034). The amount added was 1 µl of 10X GOLD buffer, 0.1 µl of PREPGEM and 8.9 µl of each well. The plate was placed in the thermocycler for a cycle consisting of 15 minutes at 75ºC and 5 minutes at 95ºC. Then, the gDNA was amplified by PCR. The reagents used were 12.5 µl of 5X Phusion HF Buffer, 2.5 µl of DNA from PREPGEM, 6.5 µl of water and 0.5 of forward and reverse primers, adding to a total volume of 22.5 µl. The PCR cycle used was the same as the one used in 2.6.2 Primer validation, with an annealing temperature of 61.8ºC.

2.8 Microfluidics System

2.8.1 Devices

The microfluidic devices and the pump (Reglo ICC, ISMATEC, Germany) used for this experiment were kindly designed and provided by Luke MacQueen, member of the Kit Parker lab of Bioengineering at the Wyss Institute. Luke designed two types of devices, the first one was a single-channeled microchip and the second microfluidic device consisted of six identical parallel microchannels. Both channel designs comprised of 5 mm width and 0.2 mm depth, made of polycarbonate and glass.

2.8.2 Cell labeling

Cells used for this experiment were HCAECs and 1016 iPSC-ECs. One hour prior to experimentation, cells were labeled with CellTracker™ Green CMFDA (C7025, life technologies). The CellTracker™ Green dye was dissolved in DMSO to a final concentration of 10 mM. The dye was then diluted in pre-warmed Serum Free Media to a final concentration of 20 µM and supplemented to the cells. Cells were incubated for 45 minutes prior to seeding in the microfluidic system.

2.8.3 Cell seeding on a microfluidic device

Microchannels were sterilized either by autoclaving or by using 70% ethanol. The day of the experiment, channels were coated with fibronectin for 2 hours at room temperature. Cells were dissociated with 0.05% trypsin (VWR) and seeded at a concentration of $1x10^7$ cells/ml. The cells were injected into the pre-coated microchannels and dispersed uniformly. The device was incubated for 4 hours at 37ºC with 5% CO_2 to allow cells to attach.

2.8.4 Shear stress

Cells were subjected to different levels of flow-induced shear stress to study gene expression. Culture medium was circulated using a peristaltic pump at 0.1 ml/min for the first 24 h for every channel. For the next 48 h, speed in every channel was increased to 0.5 ml/min, 1 ml/min and 2 ml/min. Pictures were taken every 24 h to test the viability. Shear stress was calculated by using the Purday approximation (Young, Wheeler and Simmons, 2007),

$$\tau_w = \frac{2\mu Q}{wh^2} \qquad (1)$$

τ_w is the wall shear stress, Q is the volumetric flow rate, width w = 5 mm, height h = 0.2 mm, and viscosity of the culture medium at 37ºC is μ = 0.001 Pa s.

Fluorescent images were taken 4 hours after seeding, 24 hours after exposure at 0.06 Pa, and 24 h and 48 h after exposure at 0.3 Pa, 0.6 Pa and 1.2 Pa.

2.9 Nitrate/Nitrite Fluorometric Assay

After every shear stress run, 1 ml of media was collected from every condition and the Nitrate/Nitrite content was measured by using a fluorometric Assay (780051, Cayman Chemical, USA). The assay consists of fluorometric measurement of the samples and comparison to standard values by a standard curve.

2.10 Statistical analysis

P-values below 0.05 were considered statistically significant. Statistical analyses were performed in GraphPad Prism (GraphPad Software, La Jolla, CA). All graphs in this study are shown as mean ± standard deviation (SD).

3 Results

3.1 Characterization of hPSC-ECs

The Cowan laboratory developed in collaboration with Hoffmann-La Roche, Switzerland, a rapid and efficient protocol for vascular cell differentiation. This protocol allows differentiation of hPSCs into ECs in only 6 days. This method differentiates cells in two steps, which mimics the same developmental processes occurring during embryogenesis, in which the Wnt pathway plays a critical role in mesoderm formation. When Wnt binds to its receptor Frizzled, dishevelled phosphorylates GSK3β causing β-catenin levels rise in the cytoplasm which then translocates to the nucleus allowing gene transcription. This causes an accumulation of β-catenin in the nucleus, which activates the Lef/Tcf family of DNA-binding proteins to form transcriptional complexes (Figure 8) (Sumi et al., 2008).

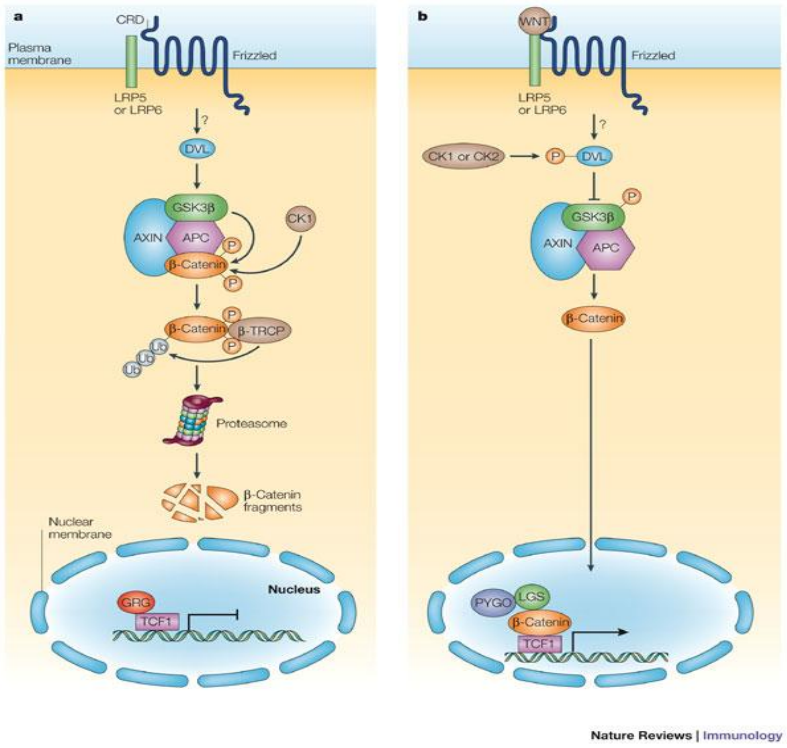

Figure 8 Wnt pathway. (a) Wnt pathway in its inactive form. Dishevelled protein is inactive which causes GSK3 complex to disrupt β-catenin. (b) Wnt pathway in its active form. Wnt binds to frizzled which causes dishevelled to inhibit the GSK3 complex allowing β-catenin translocation into the nucleus for further gene transcription (Staal and Clevers, 2005).

In the first step, CHIR-99021 (which will be referred to as CHIR for the rest of this study) and BMP4 are used to produce a mesodermal state in 4 days. CHIR is a GSK3β inhibitor leading to the constitutive activation of the Wnt pathway. On day 4, medium is changed and VEGF (a growth factor that induces angiogenesis) along with forskolin (an angiogenesis regulator) is added for 2 days. On day 6, VE-Cadherin (CD144) positive hPSC-ECs are enriched using CD144 specific magnetic beads and Magnetic Activated Cell Sorting (MACS). A schematic representation of the differentiation protocol is shown in Figure 9 (Patsch et al., 2015).

The resulting hPSC-ECs identity was confirmed by immunostaining, microarrays, and metabolic profiling. Their function was assessed by barrier function and immuno-related assays. Finally, hPSC-ECs were able to form functional blood vessels when grafted in mice (Patsch et al., 2015). In the present study, induced pluripotent cell (iPSC) line Sev-A 1016 ECs were used and Human Coronary Artery ECs (HCAECs) were used as a positive control.

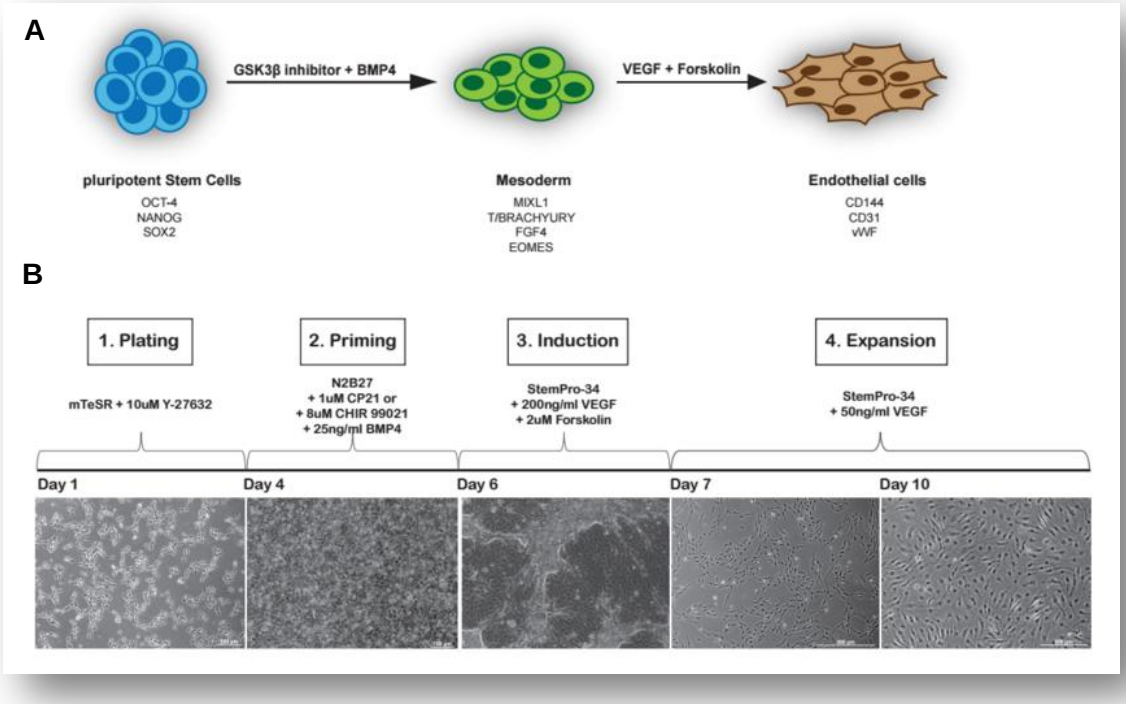

Figure 9 Flow chart of EC differentiation from hPSCs. (a) Schematic representation of the differentiation protocol with a list of the specific genes to the three major steps. (b) Timeline of critical steps of the protocol with the media and compounds used. Pictures show cell morphologies for those key steps (Challet Meylan et al., 2015).

3.1.1 Immunofluorescence Assay

The quality of the 1016 hPSC-ECs used for shear stress experiments was assessed by staining with EC specific markers. Two adhesion molecules found specifically on the membrane of ECs, VE-Cadherin (CD144), the major EC adhesion molecule which maintains vascular integrity and Platelet Endothelial Cell Adhesion Molecule (PECAM-1, CD31), a protein involved in leukocyte transmigration, were expressed on the extracellular membrane. Moreover, a glycoprotein produced by ECs von Willebrand Factor (vWF) involved in platelet adhesion for plaque formation, was located in the cytoplasm (Figure 10). DAPI staining was used to mark nuclei blue, for easier cell identification. The two adhesion molecules were expressed by a majority of the cells whereas vWF expression varied greatly from one cell to another. This heterogeneous expression was expected based on other reports and stainings on primary ECs (data not shown). In summary, immunofluorescence staining demonstrated that 1016 iPSC-ECs exhibit EC specific markers.

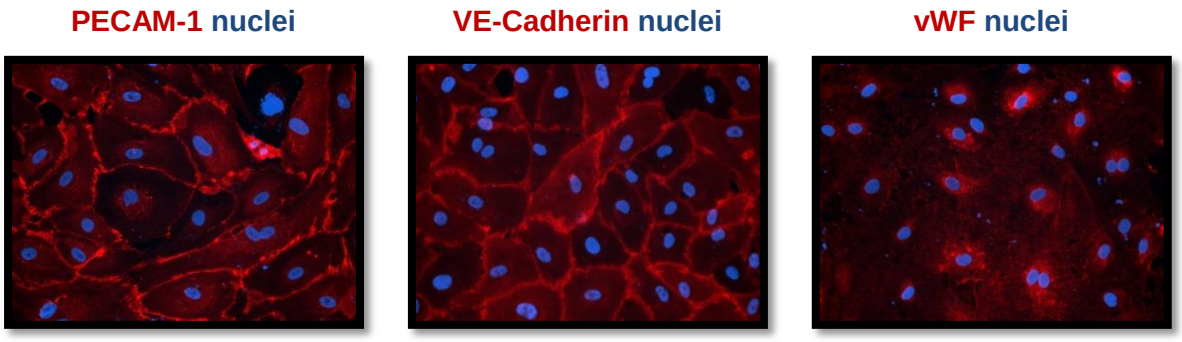

Figure 10 Immunostaining of EC specific markers on hPSC-ECs. Cells expressed PECAM-1 and VE-Cadherin, localized on the extracellular membrane, and vWF in the cytoplasm. A representative image is shown. Magnification: 20x. 1 experiment N=2 wells

3.1.2 Angiogenesis assay

ECs have the ability to form a spider web-like structure when seeded on Geltrex, a soft substrate. 1016 iPSC-ECs (passage 5) were tested for this angiogenic property using HUVECs (passage 6) as a positive control (Figure 11). Both HUVECs and 1016 iPSC-ECs formed spider web-like networks, after an overnight incubation in a thick layer of geltrex matrix.

HUVECS **1016 iPSC-ECs**

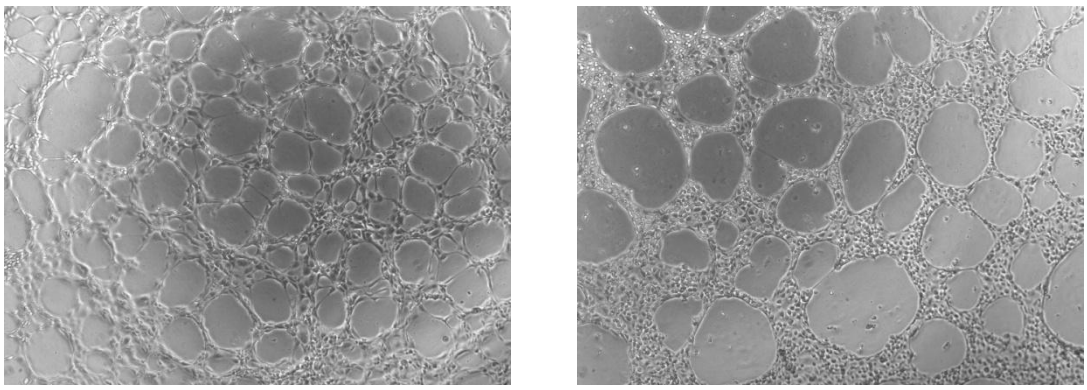

Figure 11 Angiogenesis assay on HUVECs and 1016 iPSC-ECS. Spider web-like structures were formed by ECs when seeded on a soft substrate. 1 experiment N=2 wells.

3.2 Microfluidic system set up

The microfluidic device and pump used for this experiment were kindly designed and provided by Luke MacQueen, member of the Kit Parker lab of Bioengineering at the Wyss Institute. The expertise of this lab is on cardiac cell biology and creating organs on a chip.

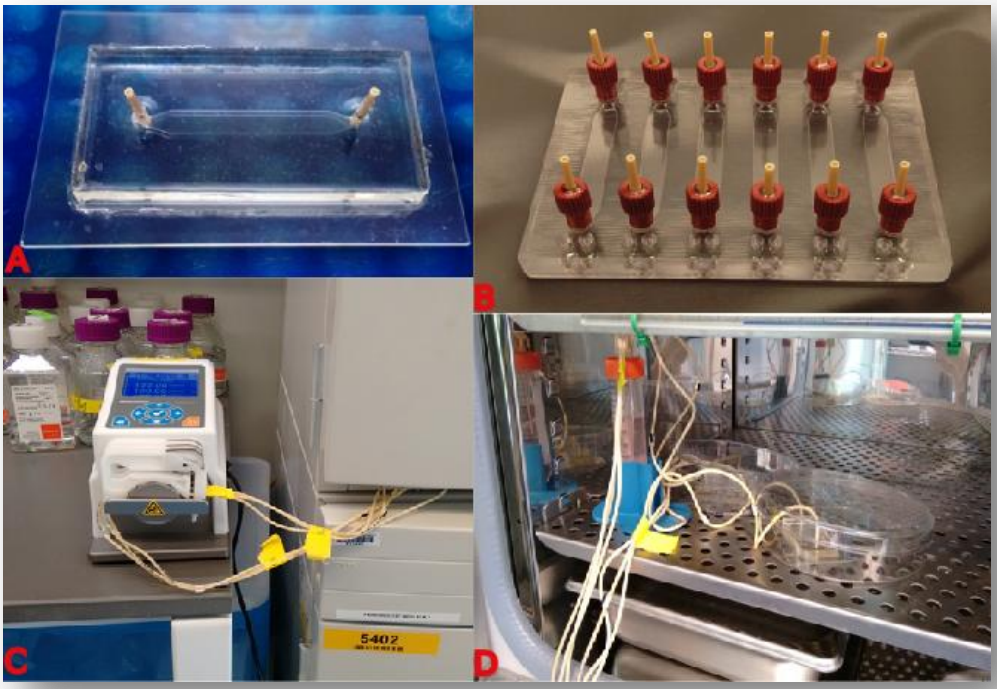

Figure 12 Microfluidic system set up. (a) Simple microfluidic channel microchip. (b) Parallel patterned microfluidic shear device, consisting of six microchannels of 5 mm width. (c-d) Example of the pump system set up inside the incubator.

Figure 12 shows an example of the two types of chips used for current (a) and future (b) experiments. Cells were injected through the nozzles inside a hood, under sterile conditions. The tubes that connected the microchip with the media supply were then joined. The falcon tube was filled with 30 ml of EGM-MV media (Figure 12(d)) and the cap was not completely closed to allow gas exchange. The tubes were then connected to the pump, which had three valves to set three different shear stress intensities simultaneously (Figure 12(c)).

3.3 Cell viability under shear stress

Preliminary experiments were designed to find the best seeding density. For better visualization under a fluorescent microscope, HCAECs were stained with CellTracker™ Green. The aim assessed if ECs could detach under the highest physiological shear stress conditions. A schematic representation of the protocol followed is shown in Figure 13.

The first set of experiments was conducted at a seeding density of $5x10^6$ cells/ml (250,000 cells/chamber). After 24 h under low shear stress (0.06 Pa), no monolayer was formed (Figure 14 (a)) and most of the cells detached after an additional 48 h under high shear stress (1.2 Pa) (Figure 14 (b)). Seeding density was therefore increased to 10^7cells/ml (500,000 cells/chamber) and different physiological shear stress conditions were tested based on previous reports (0.06 Pa, 0.3 Pa, 0.6 Pa and 1.2 Pa) (Khan and Sefton, 2010). At the new density, cells formed a monolayer and were still attached after 72 hours. Two different controls were used. The first control was kept at a static condition for approximately four hours. The second control was kept for 72 hours at low shear stress (0.06 Pa). Pictures were taken after 24 h and 48 h at different magnifications (4x and 10x) (Figure 15). At 0.6 Pa, cells started to align to the flow (arrow in Figure 15).

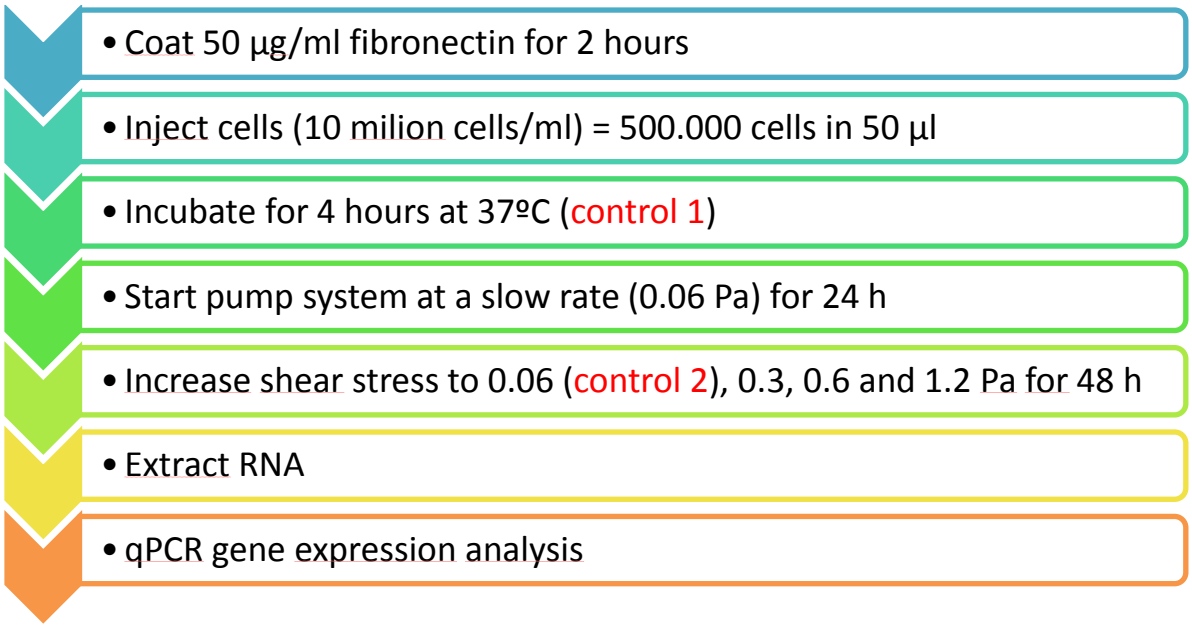

Figure 13 Schematic representation of the protocol followed to test gene expression in the microfluidic system.

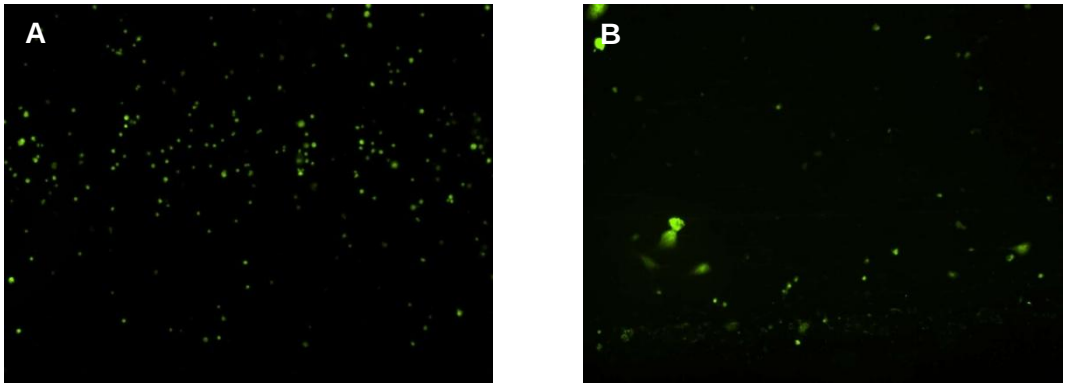

Figure 14 First experiment with HCAECs in the microfluidic system. (a) Picture taken after 24 h under low shear stress (0.06 Pa), seeding density of $5x10^6$ cells/ml. (b) Picture taken after 48 h under high shear stress (1.2 Pa), seeding density of $5x10^6$ cells/ml.

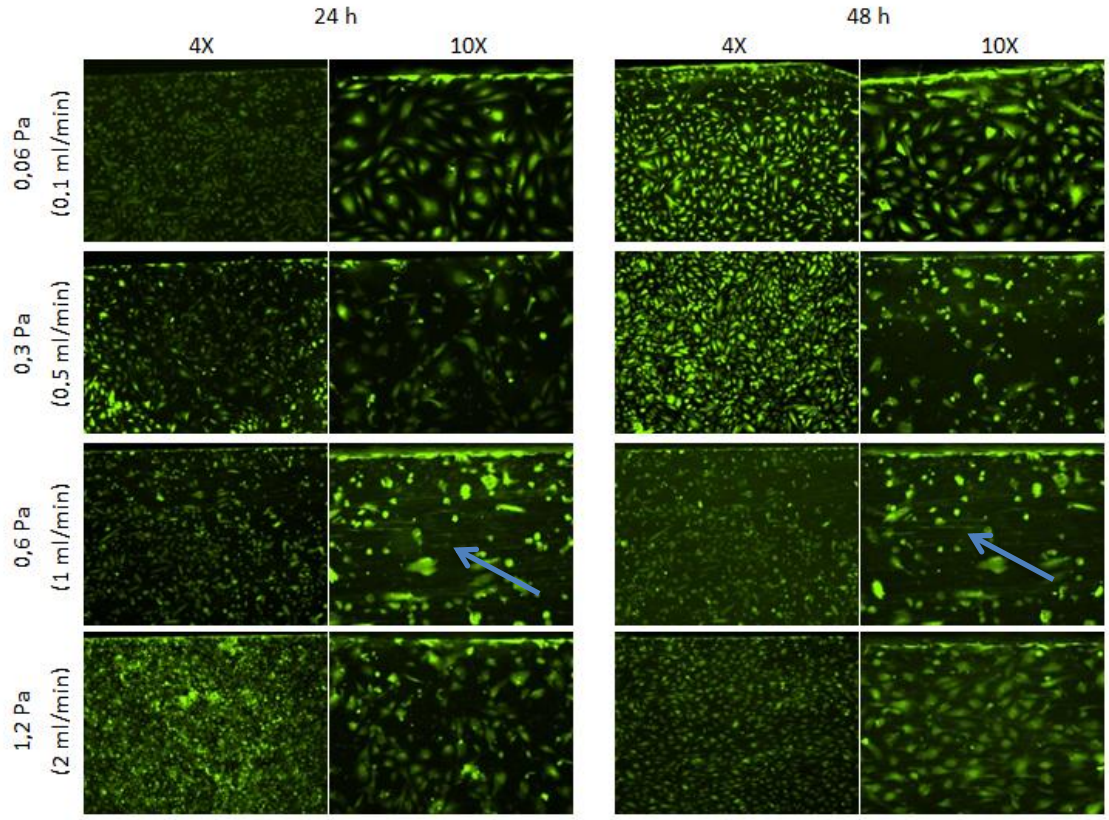

Figure 15 Second experiment with HCAECs in the microfluidic system. Seeded at a 10^7 density. Pictures taken after 24 h and 48 h at 4x and 10x. Cells were tested in four different forces (0.06, 0.3, 0.6 and 1.2 Pa). Arrow: alignment to the flow.

3.4 Gene expression under shear stress

After 48 h of cell culture under different shear stress intensities (0.06 Pa, 0.3 Pa, 0.6 Pa and 1.2 Pa), mRNA was extracted, reverse-transcribed to cDNA and tested for gene expression by qPCR. Several genes were assessed, based on the literature (Uzarski et al., 2013; Khan and Sefton, 2010). These genes are relevant for EC vascular physiology, fibrinolysis, inflammation and genes involved in the TGF-β pathway related to bleeding disorders such as Marfan syndrome and HHT. Every condition was normalized to the static and graphs were generated with the software GraphPad Prism 6. The gene expression was tested in both HCAECs and 1016 iPSC-ECs. Due to the low amount of DNA in every sample, some of the samples of the same condition were pulled together to increase the concentration. Even so, levels of the gene expression of some samples were too low to be detected by qPCR. 1016 iPSC-ECs had undetermined values for most of the CT values. Gene expression for HCAECs will be discussed first.

3.4.1 Validating the system

EC specific markers

Gene expression for EC specific factors that are constitutively expressed were tested in HCAECs (passage 5-7). PECAM-1(CD31), a protein involved in leukocyte transmigration, was expressed on the extracellular membrane (Lovelace et al., 2013). VEGFA is a growth factor active in angiogenesis, vasculogenesis and ECl growth. This growth factor induces EC proliferation, promotes cell migration, inhibits apoptosis and induces permeabilization of blood vessels (Ucuzian et al., 2010). KLF2 is a transcriptional regulator of endothelial involved in FoxO signaling pathway and embryonic differentiation pathways (De Val and Black, 2009). PECAM1 and KLF2 are higher expressed under shear stress, compared to static conditions. VEGFA levels stay rather constant under different shear stress condition compared to static condition, except at 0.3 Pa, where the expression is drastically lowered (Figure 16).

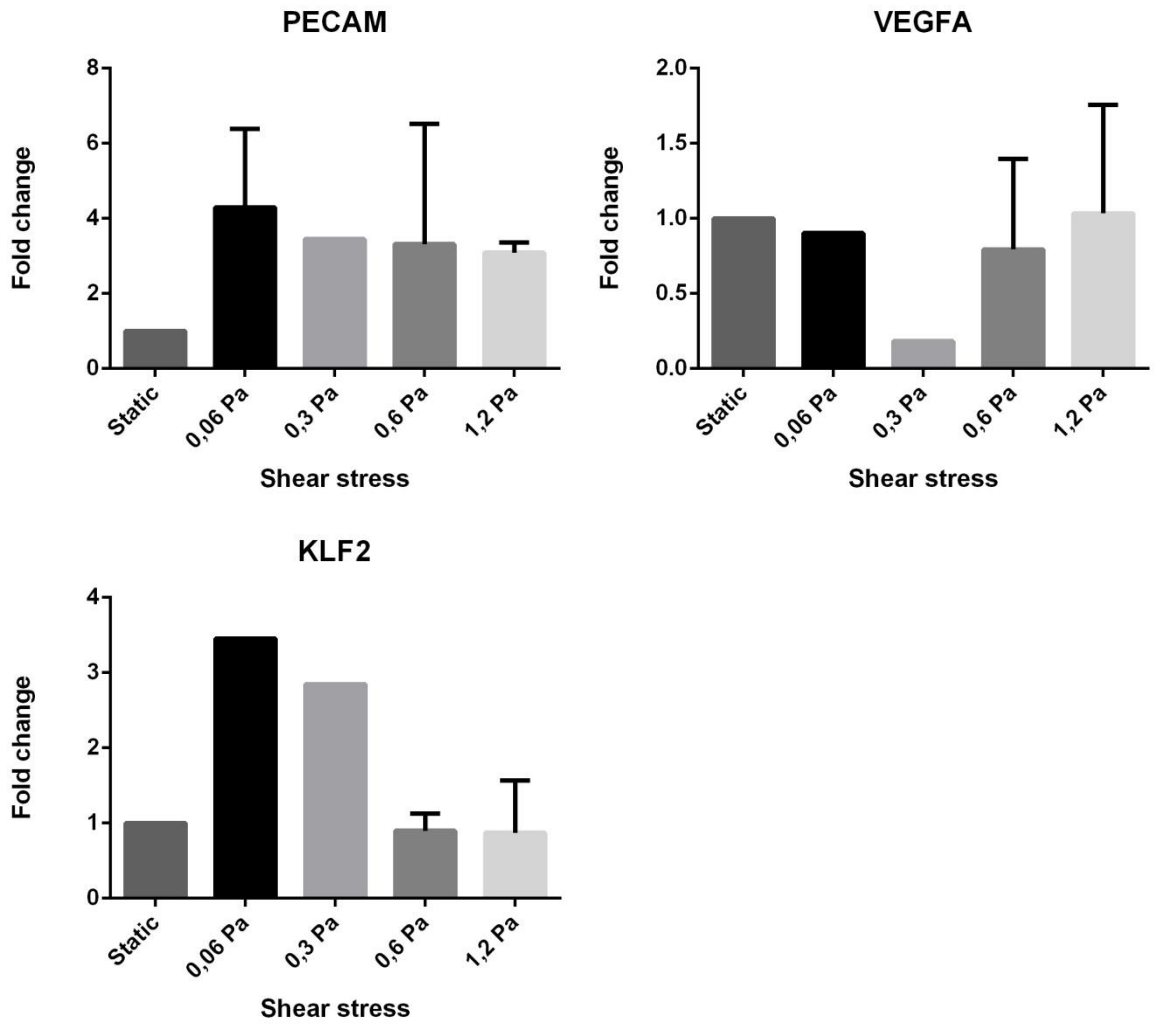

Figure 16 Gene expression of EC specific factors. Static n=1, 0.06 Pa n=5, 0.3 Pa n=4, 0.6 Pa n=4, 1.2 Pa n=4.

Adhesion molecules

ICAM-1, VCAM-1 and E-selectin (SELE) are immune system related adhesion molecules found on the surface of ECs. ICAM-1 is a surface glycoprotein that serves as a ligand for leukocyte adhesion protein LFA-1 (Ochs, Smith and Puck, 2007). VCAM-1 is a surface sialoglycoprotein expressed in ECs when they are cytokine activated. It mediates leukocyte EC adhesion and may play a role in atherosclerosis (Gawaz, 2005). E-selectin is also expressed in ECs when they are cytokine activated. It is responsible for the accumulation of leukocytes at the site of inflammation by promoting adhesion to the endothelium (Granger and Senchenkova, 2010). VCAM and SELE are in general higher expressed

under shear stress, compared to static conditions, whereas ICAM is down regulated when exposed to shears stress, with a down regulation maximum at 0,03 Pa (Figure 17).

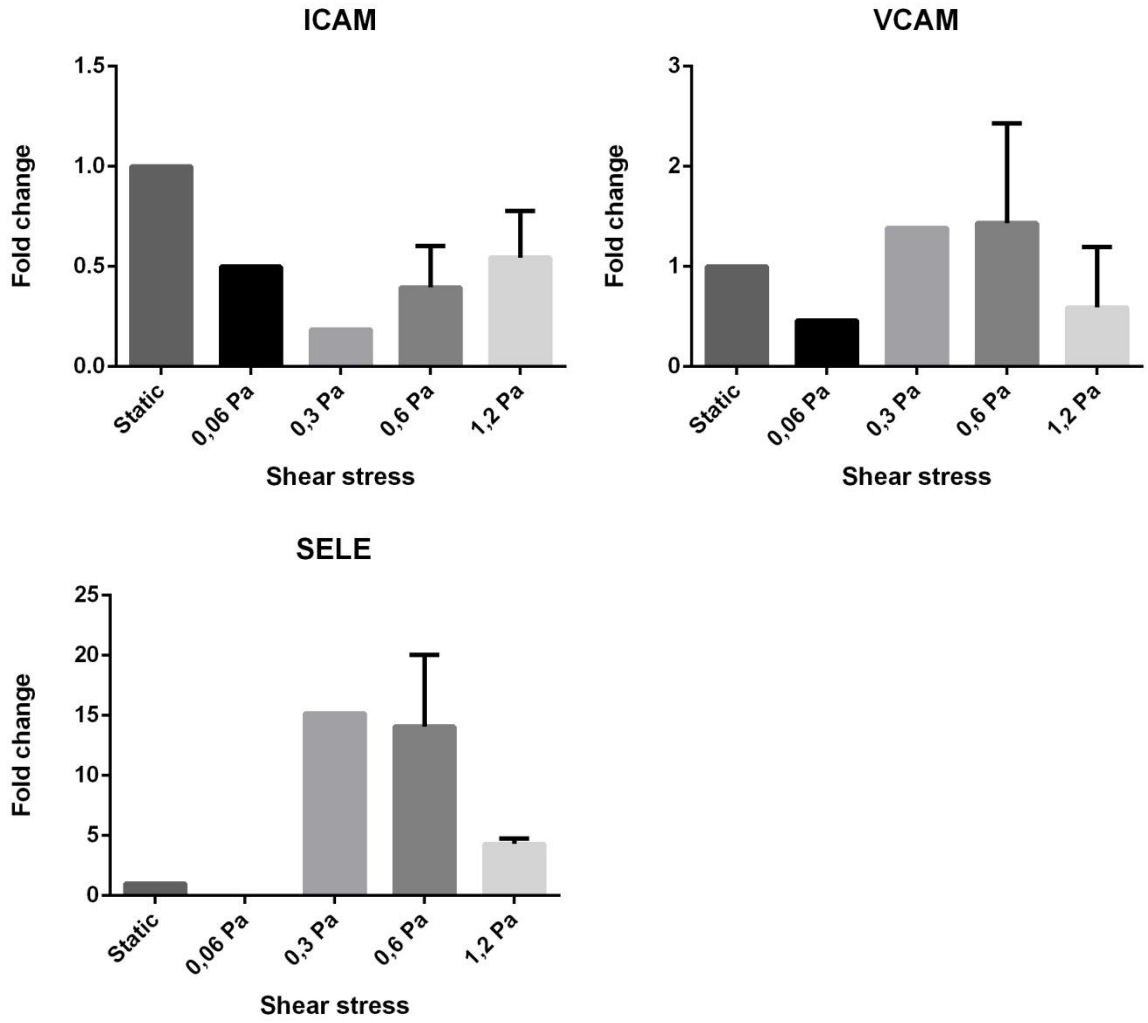

Figure 17 Gene expression of EC associated adhesion molecules and factors. Static n=1, 0.06 Pa n=5, 0.3 Pa n=4, 0.6 Pa n=4, 1.2 Pa n=4.

Inflammation associated gene expression

ECs create a barrier which is of great importance during extravasation of immune cells. Expression for inflammation associated genes (PLA2G4C, ADAM17 and CX3CL1) was measured. PLA2G4C is a member of phospholipase A2 enzyme family, involved in the process of producing free fatty acids and lysophospholipids that serve as precursors in the production of signaling molecules (Ncbi.nlm.nih.gov, 2016). ADAM17 is an enzyme that mediates TNF-a shedding from the cell membrane (Tsou, 2001). CX3CL1 is a fractalkine

which has a role in chemotaxis, adhesion of leukocytes and supports the survival of multiple cell types during homeostasis and inflammation (White and Greaves, 2012). All three inflammation associated genes show downregulation at 0.06 Pa, but suffered a drastic upregulation under higher levels of shear stress (Figure 18).

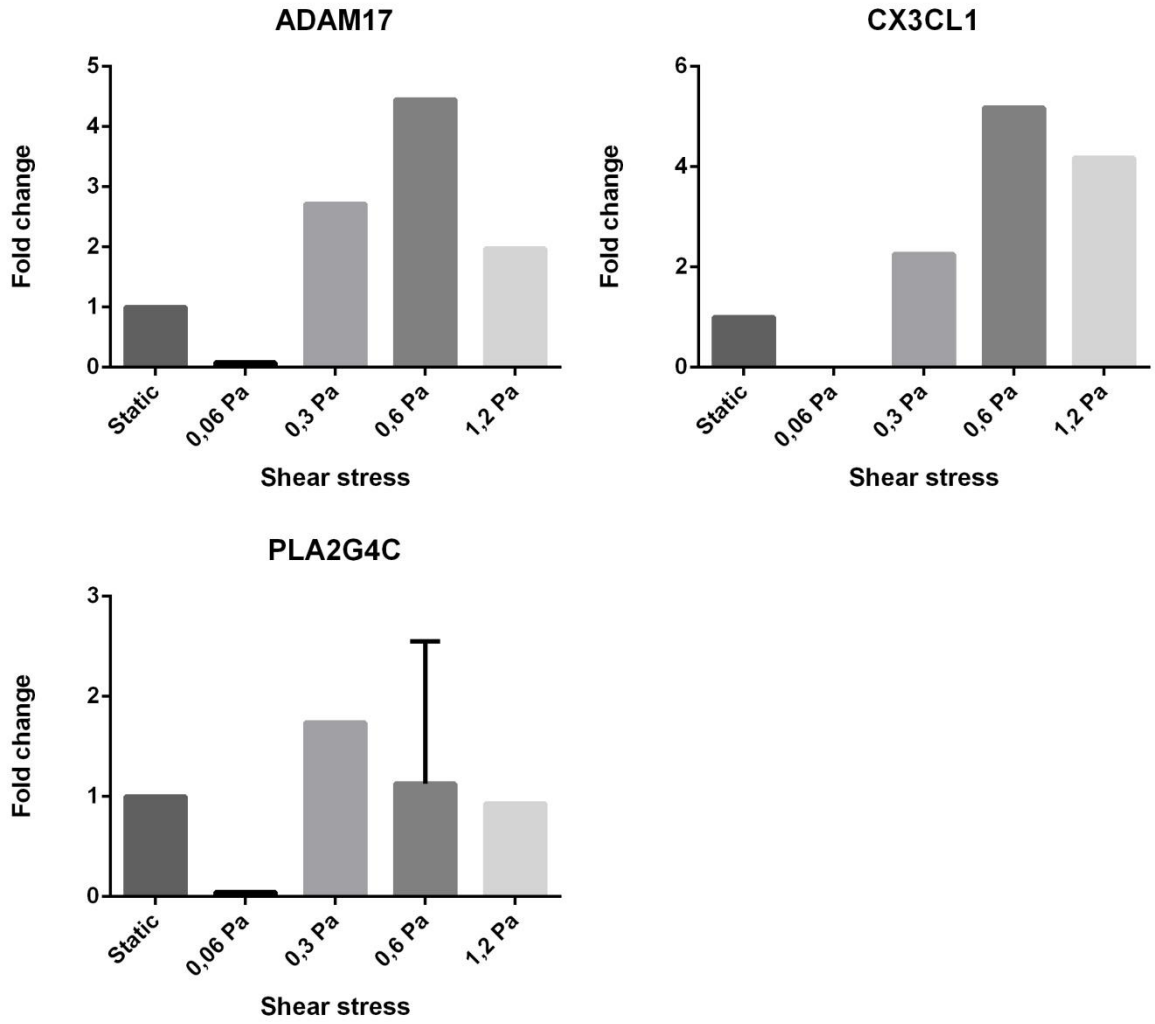

Figure 18 Inflammation related gene expression. Static n=1, 0.06 Pa n=5, 0.3 Pa n=4, 0.6 Pa n=4, 1.2 Pa n=4.

Cardio-protective gene expression

Genes relevant in vascular physiology which are standard clinical diagnostic markers of CVD were assessed next. Endothelin-1 (EDN1) is a vasopressive gene which causes smooth muscle cell contraction. It is also involved in atherosclerosis (Ncbi.nlm.nih.gov, 2016). Superoxide dismutase-1 (SOD-1) is an enzyme protective against oxidative stress (Figure 19) (MatÉs, Pérez-Gómez and De Castro, 1999). EDN1 shows highest expression

at 0.6, intermediate expression at 0.3 and 1.2 Pa, and an expression minimum at 0.06 Pa. Compared to that, SOD1 expression is the highest at 0.3 Pa. Intermediate expression of SOD1 occurs at 0.6 and 1.2 Pa, and as in EDN1 the expression minimum is at 0.06 Pa.

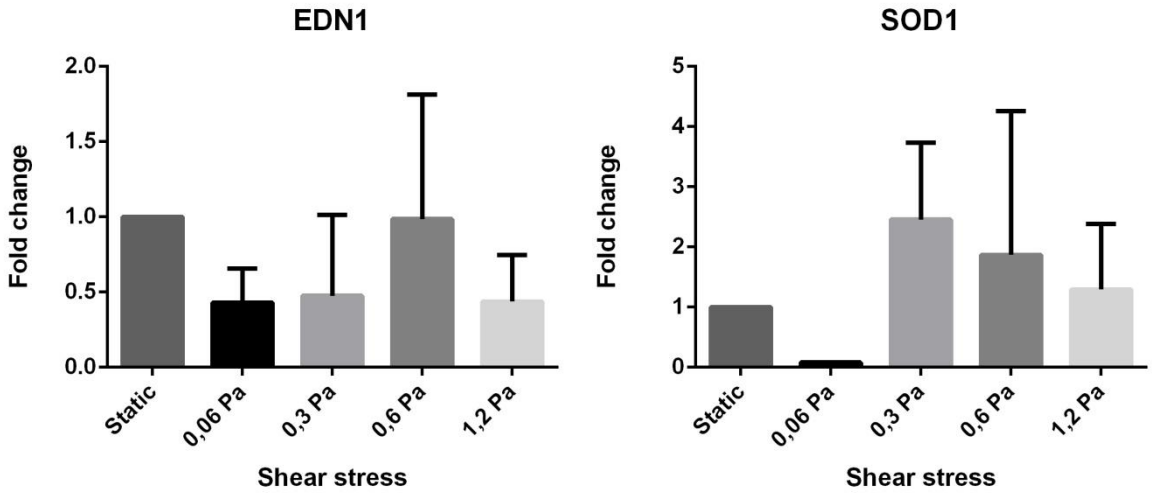

Figure 19 cardio-protective gene expression. Static n=1, 0.06 Pa n=5, 0.3 Pa n=4, 0.6 Pa n=4, 1.2 Pa n=4.

Coagulation and fibrinolysis associated genes

Furthermore, coagulation (formation of a clot when a blood vessel is disrupted) and fibrinolysis (disintegration of clots in blood vessel) associated gene expression was studied. ANXA5 is a plasma protein with anticoagulant properties (Rand et al., 2009). PLAU is a plasminogen activator (Ncbi.nlm.nih.gov, 2016). ANXA5 shows little down regulation at 0.3 and 0.6 Pa, and was drastically down regulated at 1.2 and 0.06 Pa. On the other hand, PLAU is downregulated under all different shear stress conditions (Figure 20).

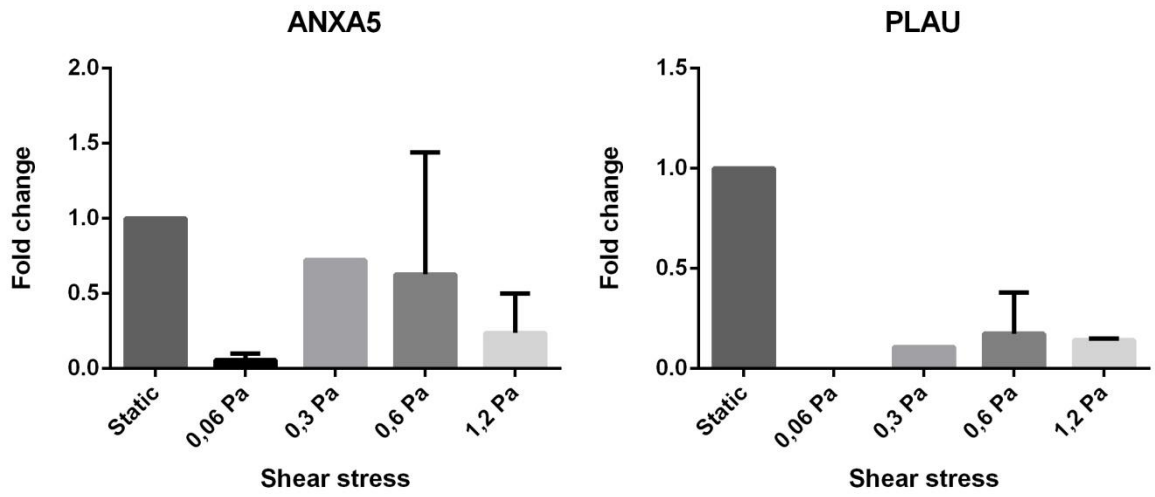

Figure 20 Coagulation and fibrinolysis associated gene expression in HCAECs. Static n=1, 0.06 Pa n=5, 0.3 Pa n=4, 0.6 Pa n=4, 1.2 Pa n=4.

3.4.2 Disease related gene expression

Marfan syndrome and HHT

Once the system was validated, gene expression of the disease related genes was tested. Figure 21 shows the gene expression of KRIT1 and ENG in HCAEC, genes involved in HHT which cause malformations in the brain blood vessels (Whitehead, Smith and Li, 2012). Both KRIT 1 and ENG expression increases with increasing shear stress, and show a big drop in expression at 1.2 Pa.

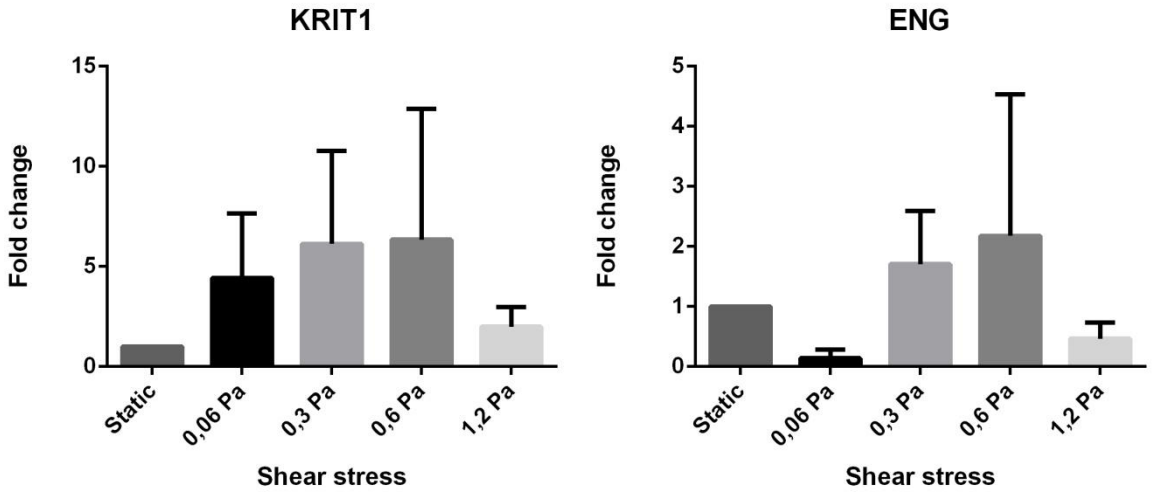

Figure 21 HHT and Marfan syndrome related gene expression. Static n=1, 0.06 Pa n=5, 0.3 Pa n=4, 0.6 Pa n=4, 1.2 Pa n=4.

CVD

Figure 22 shows genes implicated in CVD at the 9p21.3 locus. CDKN2A and CDKN2B are two cell cycle regulating genes reported to be regulated by ANRIL (Pasmant et al., 2007). CDKN2B gets increasingly upregulated at 0.06 and 0.3 Pa, and shows almost no change in expression at 0.6 and 1.2 Pa, compared to static conditions, whereas CDKN2A shows an expression maximum at 0.06 Pa, an expression minimum at 0.3 Pa, and almost no change in expression at shear stress of 0.6 Pa or higher.

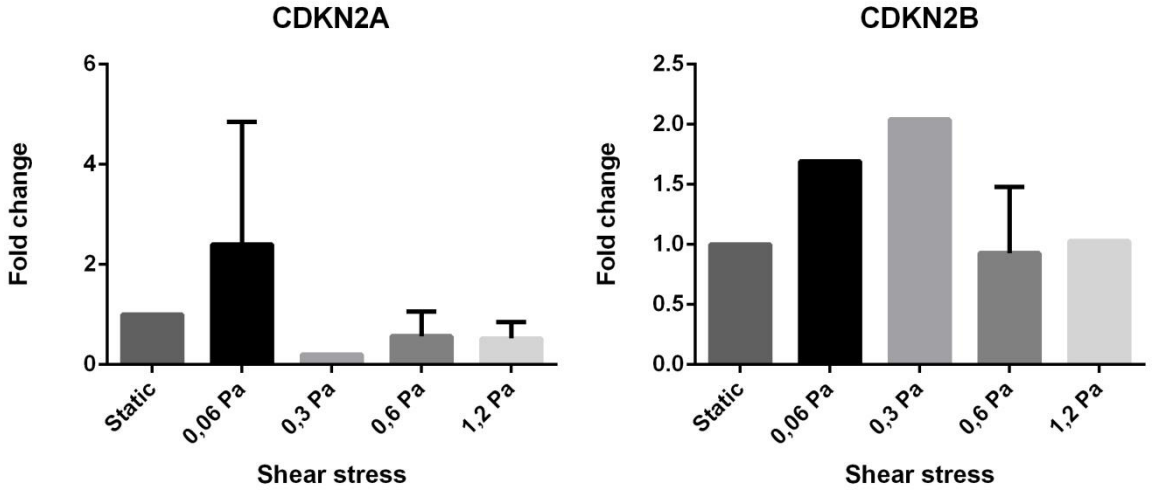

Figure 22 Gene expression of genes related to ANRIL in HCAECs. Static n=1, 0.06 Pa n=5, 0.3 Pa n=4, 0.6 Pa n=4, 1.2 Pa n=4.

3.4.3 Gene expression in iPSC-ECs

The same gene expression test was performed with iPSC-ECs. Very few genes were expressed enough to be detected. Figure 23 shows the gene expression of the expressed genes, which were the adhesion molecules PECAM and ICAM, the protective gene against oxidative stress SOD-1, vasopressive gene which causes smooth muscle cell contraction EDN1, HHT related ENG and AKT2. PECAM and SOD-1 are hardly expressed, whereas AKT2 and ICAM are highly expressed compared to static. EDN1 is downregulated at physiological levels. ENG is upregulated at low shear stress levels and drastically downregulated at higher ones.

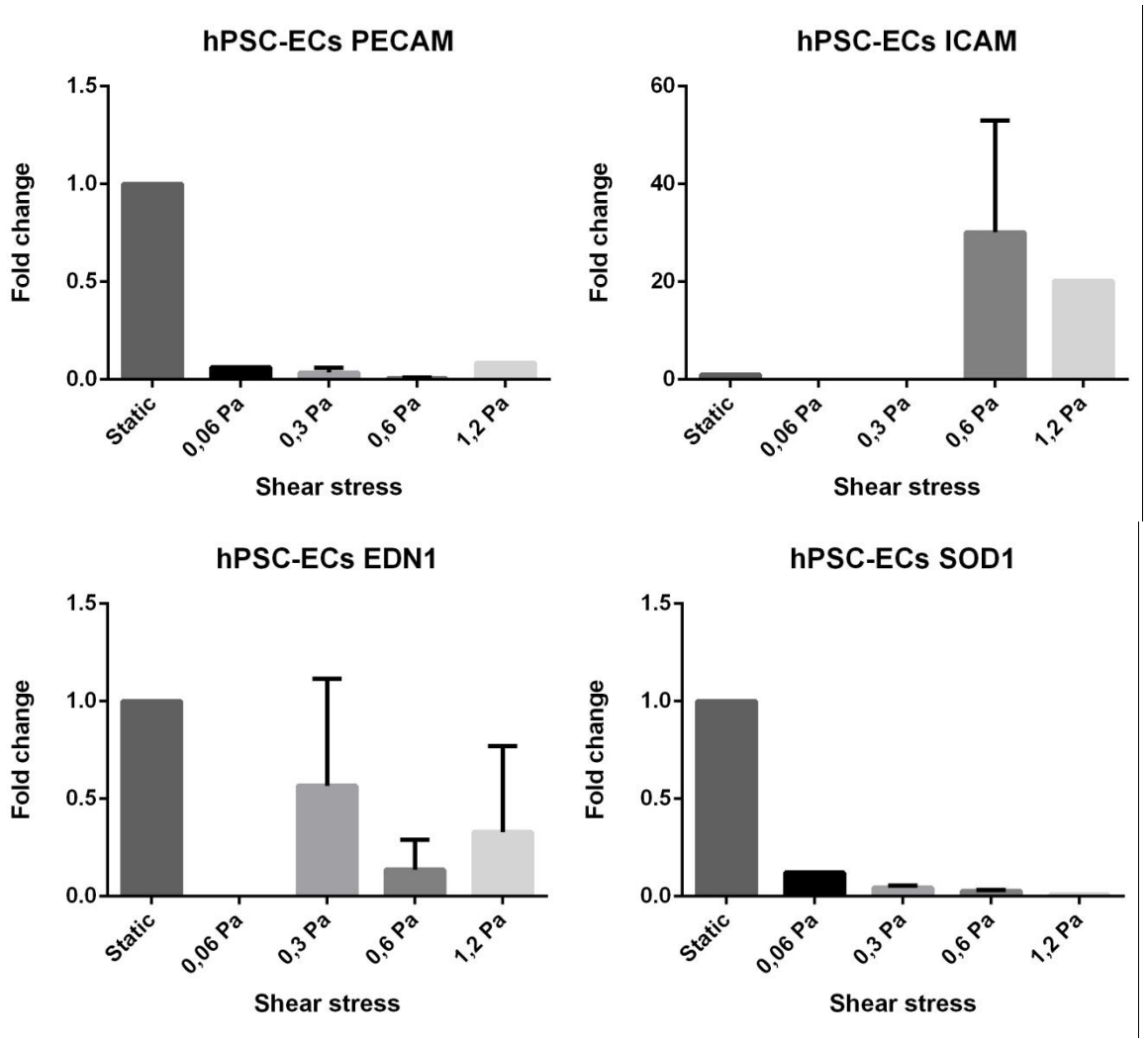

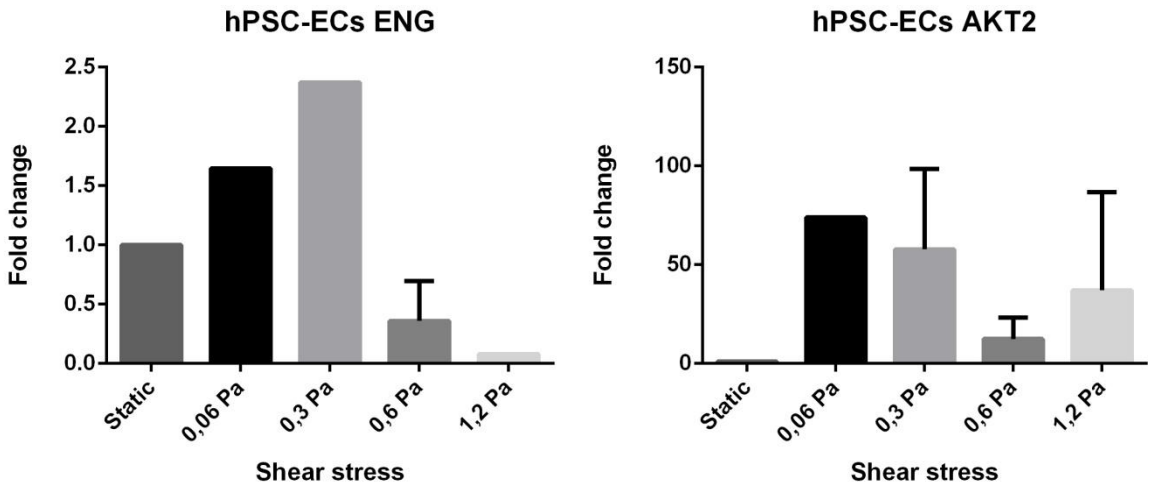

Figure 23 Gene expression in 1016 iPSC-ECs. Static n=1, 0.06 Pa n=2, 0.3 Pa n=3, 0.6 Pa n=3, 1.2 Pa n=2.

3.5 eNOS function

Endothelial nitric oxide synthase (eNOS) is an enzyme involved in the production of nitric oxide. This enzyme is constitutively expressed and is highly regulated in ECs. Nitric oxide has an important function in the inhibition of leukocyte adhesion, platelet aggregation and smooth muscle cell proliferation. The function of nitric oxide is of great importance because it allows an uninterrupted flow of blood through the vessels (Pahakis et al. 2007). qPCR results show that eNOS was highly expressed at low shear stress (0.3 Pa) and downregulated at higher shear stress levels (Fig 24(a)). The Nitrate/Nitrite concentration in the media was quantified by a fluorometric assay (Fig 24(b)). The graph shows a dramatic increase in Nitrate/Nitrite production at high shear stress levels for both HCAECs and 1016 iPSC-ECs. The lowest concentration found in HCAEC is at 0.3 Pa, whereas for 1016 iPSC-ECs is at 0.6 Pa.

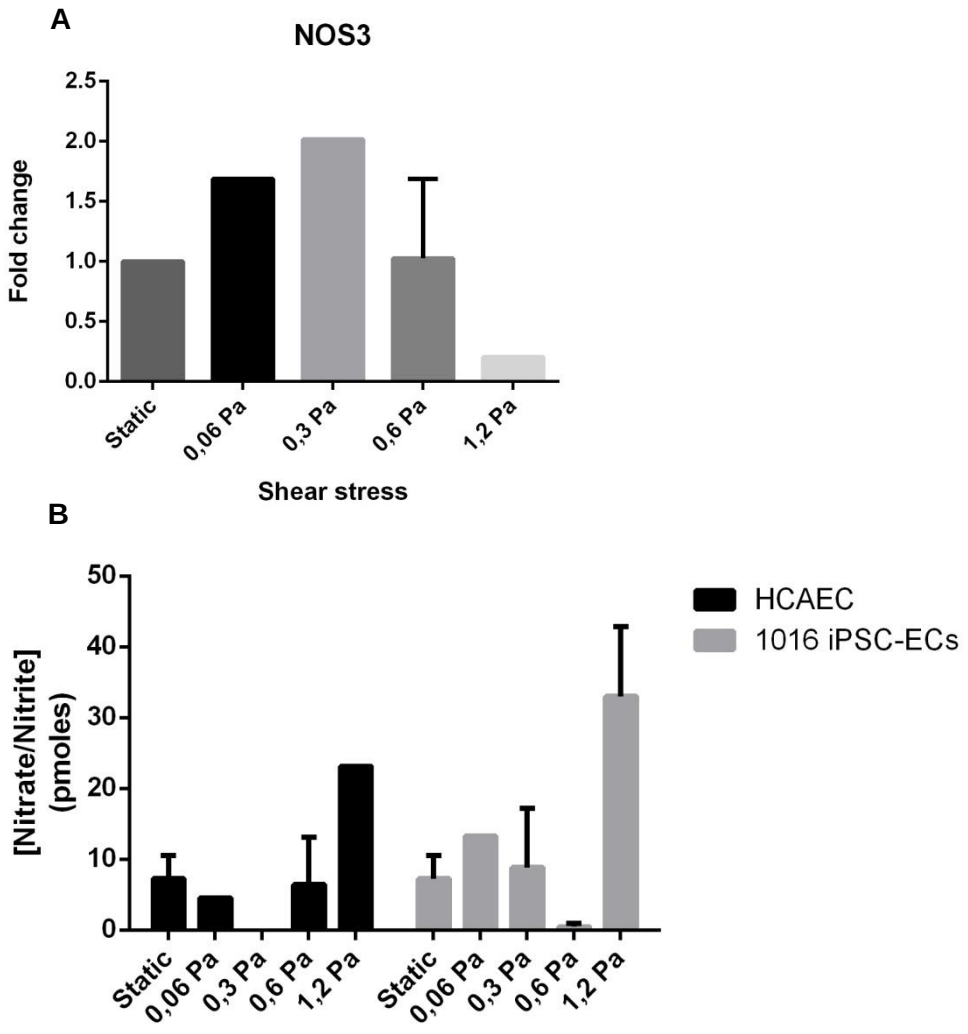

Figure 24 eNOS function. (a) eNOS gene expression in HCAEC. Static n=1, 0.06 Pa n=5, 0.3 Pa n=4, 0.6 Pa n=4, 1.2 Pa n=4. (b) Nitrate/Nitrite (pmoles) concentration in media. Represented are both HCAECs (Static n=1, 0.06 Pa n=1, 0.3 Pa n=1, 0.6 Pa n=4, 1.2 Pa n=1) and 1016 iPSC-Ecs (Static n=1, 0.06 Pa n=1, 0.3 Pa n=2, 0.6 Pa n=2, 1.2 Pa n=2). N=3 wells per concentration.

3.6 CCL7 targeting using CRISPR/Cas9 system

The CRISPR/Cas9 technique was used to knock out CCL7, in order to use the cells in the shear stress system. The main function of CCL7 chemokine is to attract macrophages, monocytes and eosinophils during inflammation and metastasis (described in section 1.3). Based on what is known about inflammation related genes and shear stress, it would be interesting to study gene expression of CCL7 in these conditions.

3.6.1 CRISPR and primer design

In the CRISPR technology, a dual guide strategy was implemented. This involves designing two CRISPR guides which create a deletion in the DNA of interest. The NCBI database was used to retrieve the human genomic sequence of CCL7 and five sgRNA sequences were designed by using MIT CRISPR design tool. Four screening primers flanking the excision region were designed in NCBI primer blast (Sequences are shown in table 4 in section 2.5.1). Figure 25 shows a screen capture of the APE software with highlighted sequences for sgRNAs and primers.

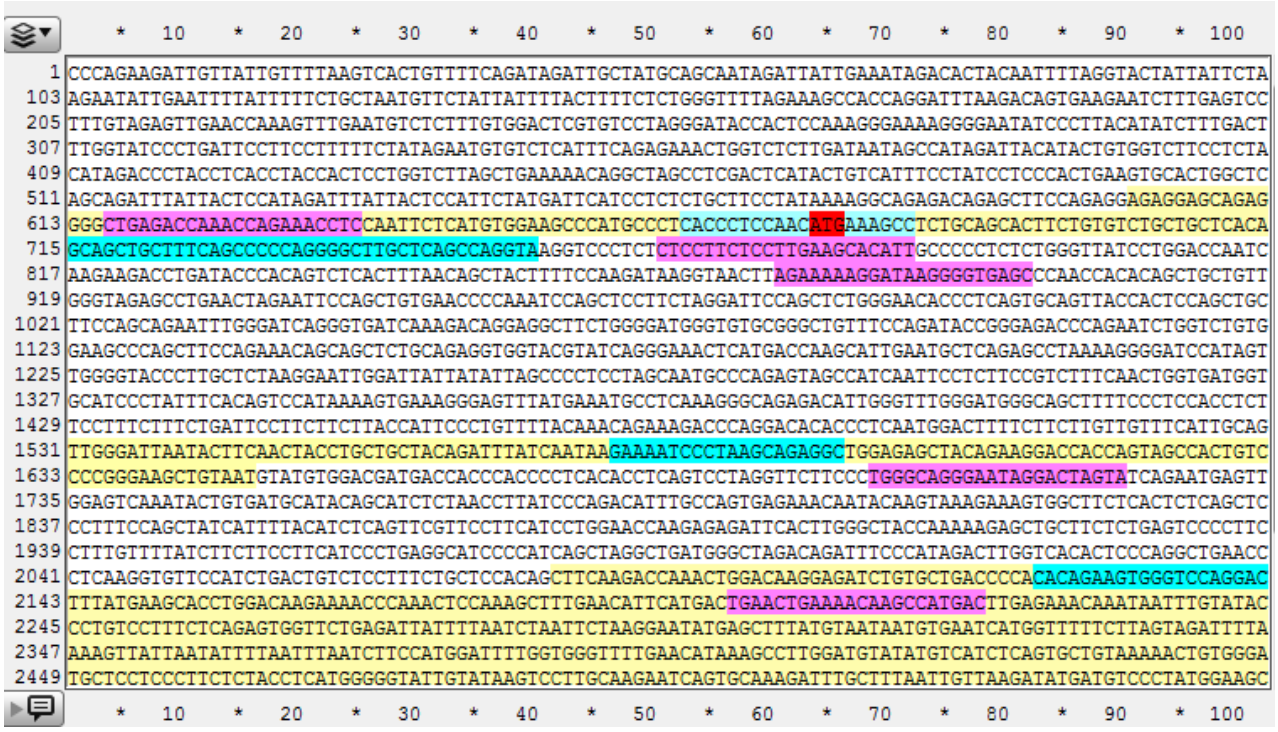

Figure 25 APE software screen capture containing CCL7 genomic sequence. Yellow: Exons; Red: start codon; Blue: sgRNA sequence; Purple: screening primer.

3.6.2 Primer validation

Primers for clone screening were validated by performing a gradient PCR with extracted gDNA from Sev-A 1016 IPSCs. The PCR annealing step was set to vary from 50ºC to 70ºC. Based on the results, temperatures from 55.5ºC to 68.4ºC were appropriate. A temperature of 61.8ºC was chosen because it is the annealing midpoint (Figure 26).

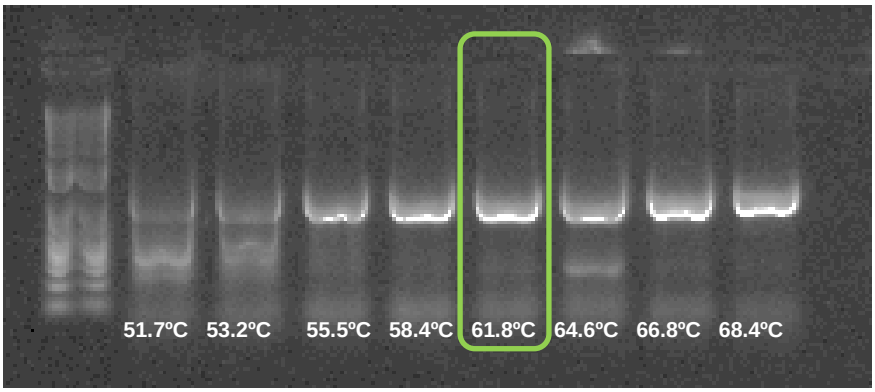

Figure 26 Gradient PCR of the primers. Temperature selected was 61.8 ºC.

3.6.3 CRISPR testing in 293T cells

CRISPR oligos were annealed, phosphorylated and ligated. After sgRNA was transformed into E. coli, the plasmid was extracted and transfected into 293T cells to test which combination of CRIPSR result in a deletion and what pair is the most efficient. Figure 27 shows a schematic representation of the position of the CRISPRs. Figure 28 is a picture of a gel were the band sizes of different combinations are shown.

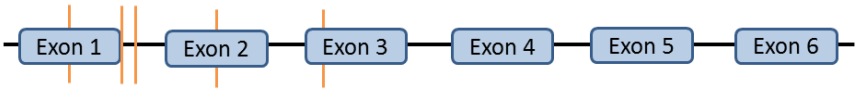

Figure 27 Schematic representation of CCL7 gene and the position of the designed CRIPSRs. CRISPRs are represented as a yellow vertical line.

Table 5 Expected band sizes

CRISPR pair	Band size (bp)	CRISPR pair	Band size (bp)
1/4	892	1/5	1438
2/4	842	2/5	1388
3/4	822	3/5	1368
		4/5	526

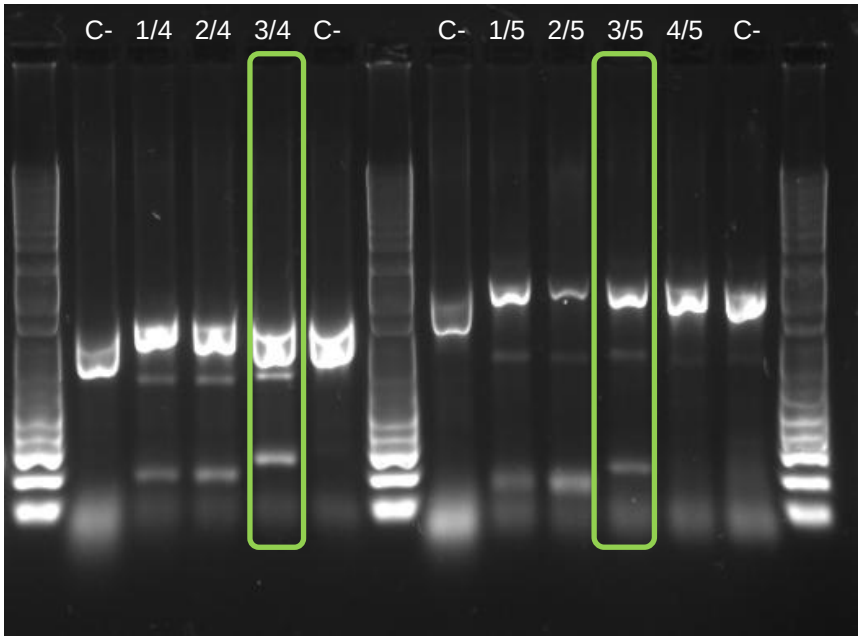

Figure 28 Isolated clones from 293T cells. First set of bands: combination of CRISPRs 1, 2 and 3 combined with 4. Second set of bands: CRISPRs 1, 2 and 3 combined with 5. First row: negative control performed with Sev-A 1016. Last row: negative control performed with untransfected 293T cells.

3.6.4 Electroporation and cell sorting

Once the best CRISPR combinations were determined, they were electroporated into 293 T Cells using transfection reagent PEI. Approximately, 10^6 cells were sorted by FACS after 48 h. Fluorescence pictures were taken 48 hours after electroporation (Figure 29). Figure 30 shows graphs taken during cell sorting. The gate shows the GFP expressing cells in blue, the gating was very restrained because highly expressed GFP cells were selected (1.2%). Graph A shows forward scatter against side scatter to measure size and granularity respectively. Graph B shows fluorescence analysis analyzed by Phycoerythrin (PE) against GFP fluorophores. Cells were re-plated in a 10 cm^2 plate in condition media, which contains 50:50 ratio of new and recycled media.

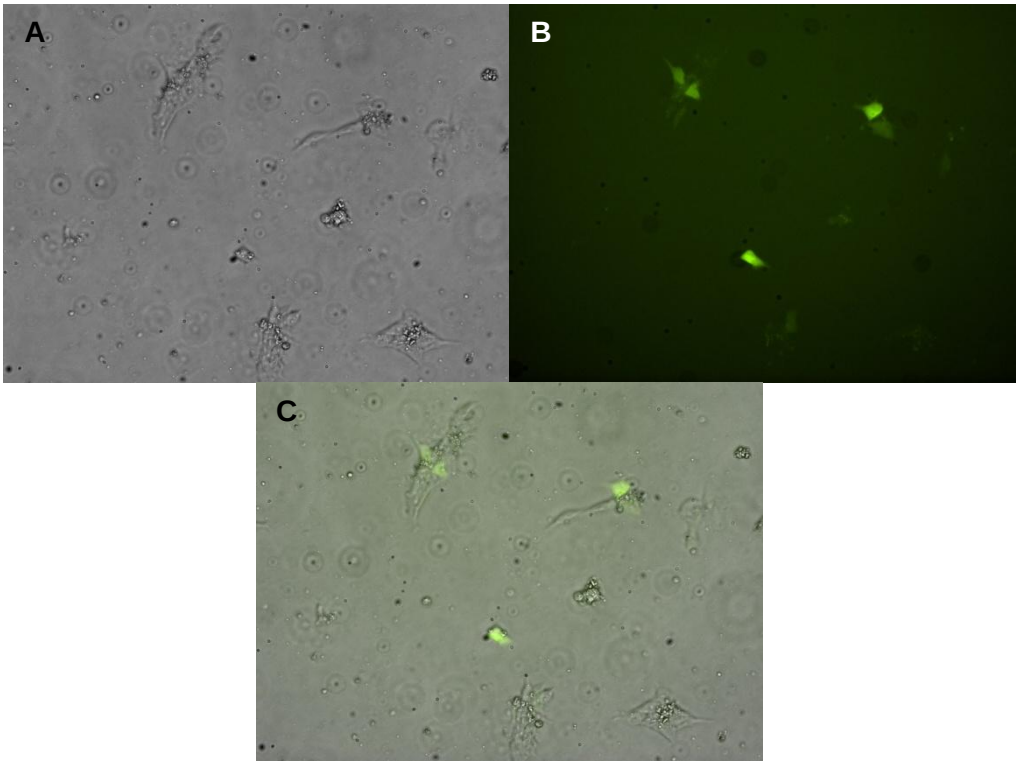

Figure 29 Electroporated cells. Fluorescent pictures were taken 48 hours after electroporation. (a) Bright field (b) FITC (c) merged (magnification 4X).

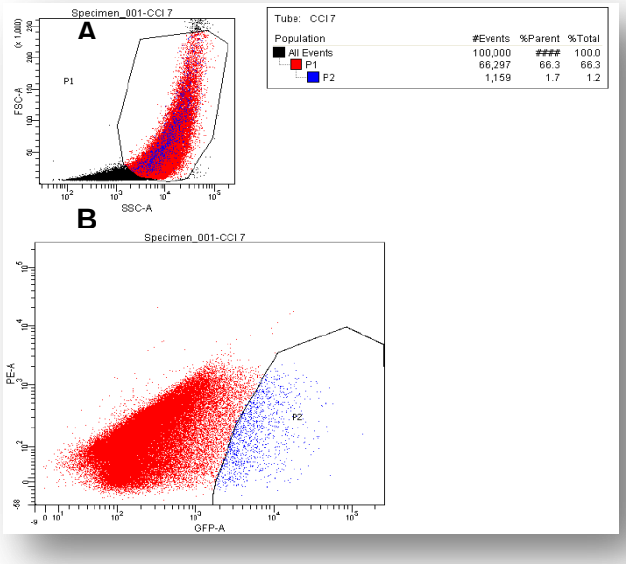

Figure 30 Fluorescence-activated cell sorting on electroporated cells. Electroporated cells shown in blue. (A) shows forward scatter vs. side scatter measuring size and granularity. (B) shows Phycoerythrin (PE) vs. GFP.

3.6.5 Clone screening

Colonies were monitored closely. When they reached the size of approximately a dime, they were picked and plated in a 96-well plate. An example of an adequate colony and a deficient colony is shown in Figure 31(a). After 3-5 days, the cells were split into three plates, one as a backup, the second one was used for gDNA extraction. The third one was frozen and kept as stock. Each well was screened to test which clones were a complete knock out, which were heterozygous, and which were wild type. In Figure 31(b), three lanes are marked which contain a homozygous, wild type and heterozygous respectively.

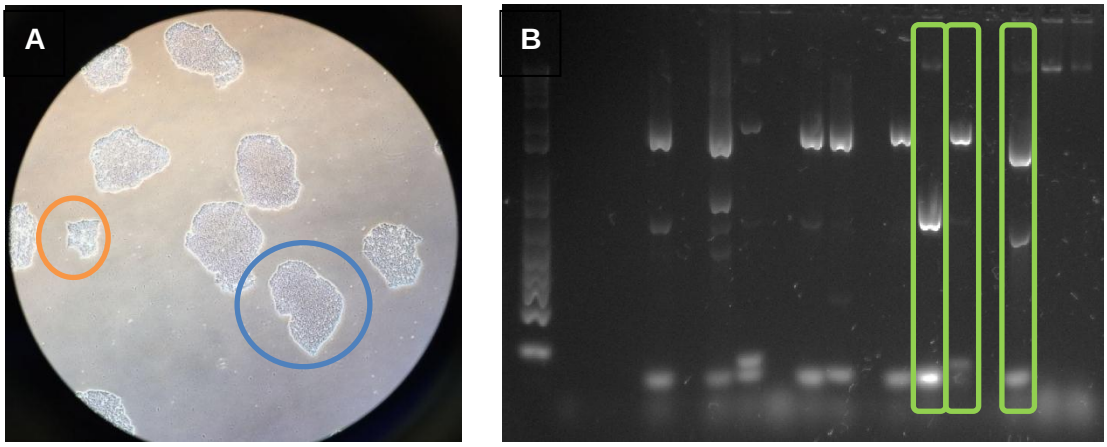

Figure 31 Clone screening. (a) Colonies of electroporated and sorted cells. Blue circle shows an adequate colony. Orange circle shows a deficient colony. (b) Clone screening. The first marked lane contains a homozygous clone, the second marked lane contains a wild type clone and the third marked lane contains a heterozygous clone.

4 Discussion

Cardiovascular disorders are a group of disorders affecting the heart and vascular system. They are a significant global burden currently causing 17.5 million annual deaths, representing 30% of all deaths in the world (WHO, 2016). There have been extensive studies on CVD but still remain significant gaps in knowledge surrounding normal signaling processes and abnormal development results remain.

A way to study this processes is to create disease models. Mice are a common accessory to model diseases. However, CVDs are not able to be reproduced in mice due to the genetic differences (Zaragoza et al., 2011). A better approach is to model diseases in cells *in vitro*. Generating mutant clones and differentiating them has become a simple and reproducible task. CRISPR/Cas9 is a novel technique that is already causing a breakthrough in research for disease modeling due to its simplicity and great advantages in genome engineering (Barrangou, 2012).

Several reports and personal observations in the Cowan lab suggest that hPSCs-derived cells do not always recapitulate the gene expression patterns observed *in vivo*. This could in part be explained by the fact that differentiated cells do not receive signals from proteins transported by the blood, mechanotransduction or interactions with neighboring cells. This is the main issue for disease modeling, where genes are not expressed in a simple culture dish. Shear stress application was chosen for this study as a better way to model disease.

In this project, a tool was implemented to apply shear stress on ECs with the purpose of creating a more accurate disease model. The differences in gene expression at different shear stress rates were investigated in the hope of better understanding the causes and mechanisms of CVD complications in the vascular system.

Functional tests (Figure 9-10) showed that hPSC-ECs behave similarly to primary ECs, as described by Patsch et al (2015). Immunofluorescence performed on 1016 iPSC-ECs stained for EC specific markers, namely, VE-Cadherin (CD144) and Platelet Endothelial Cell Adhesion Molecule (PECAM-1, CD31) found on the extracellular membrane, and von Willebrand Factor (vWF), located in the cytoplasm. Moreover, the 1016 iPSC-ECs successfully formed spider web-like structure, confirming their angiogenic potential (Figure 10). Therefore, it can be concluded that 1016 iPSC-ECs behave as ECs and are competent to be used for shear stress experiments.

Shear stress is the key to the regulation of vascular structure. Signaling pathways include nitrogen oxide and radicals derived from oxygen as well as other signs of mediation. The role of radicals derived from oxygen becomes dominant in cases in which the shear stress

changes rapidly or has a pulsatile component. This is due to activation of different shear stress sensors depending on the type of flow and activation of various routes of reactive oxygen species (Pahakis et al. 2007).

There were two controls used for the microfluidic system experiment. The first control consisted of static cells that were incubated for four hours in the chamber. The second control was kept for 72 hours under low shear stress. The chamber has a capacity of 50 µl of medium which is not enough for the viability of the cells at static conditions. Therefore, a low shear stress level (0.06 Pa) was used.

In response to the laminar flow, cells are capable of elongating in the direction of flow (Pahakis et al. 2007). In Figure 15, cells show an alignment to laminar flow at 0.6 Pa indicating that 0.6 Pa is the reliable intensity of this microfluidic system. Figure 21 shows a maximum expression at 0.6 Pa of genes related to Marfan syndrome and HHT, which suggest that this one is the ideal condition for disease modeling.

A particular point of interest our data emphasizes, is the effect of hypertension in development of CVD. Given that the pro-inflammatory mRNA expression levels in primary ECs which were upregulated in 0.6 pascal conditions, we could hypothesize the 0.6 pascal is the key stress hydrodynamic flow in ECs. In addition, the presence of inflammation stimulates ECs to exhibit elevated levels of endothelial adhesion molecules such as VCAM1 and E-selectin. This increases the responsiveness of ECs to inflammation demonstrated by the upregulation of inflammation-related genes ADAm17, CX3CL1 and PLA2G4C (Figure 18). This leads to a vicious cycle of chronic inflammation of the vascular system, which contributes to permanent endothelial dysfunction, and eventually leads to cardiovascular pathogenesis and associated co-morbidities. PECAM1 which is constitutively expressed in ECs with a similar level is also known to play a critical role in the regulation of inflammatory response. However, recent studies discovered that PECAM1 serves various pro-inflammatory as well as anti-inflammatory functions (Privratsky et al., 2011). Moreover, it could be shown that it is involved in leukocyte trans-endothelial migration, but contrastingly also is able to induce leukocyte activation and can suppress pro-inflammatory cytokine production.

When all the data of HCAEC expression is examined, cellular processes can be seen. For instance, there is evidence that KLF2 plays a key role in generating atheroprotective effects by inducing eNOS expression and inhibiting expression of E-selectin and VCAM-1 (SenBanerjee et al., 2004). Figure 16 shows an upregulation of KLF2 at 0.06 Pa which induced the downregulation of VCAM-1 and E-selectin (Figure 17) at 0.06 Pa. Moreover, eNOS was upregulated at the same condition (Figure 24). This facts correlate with the theory explained above.

When comparing this study with Uzarski et al. (2013), there seem to be some differences in expression that could be due to cell type used. HCAECs isolated from arteries were used for this study, whereas HUVECs were used for Uzarski et al. (2013). VCAM-1 and E-selectin were downregulated under physiological flow in HUVECs, while in HCAECs they were upregulated (Figure 17). ICAM was upregulated in HUVECs and downregulated in HCAECs. In the case of inflammatory associated genes PLA2G4C, ADAM17 and CX3CL1, they were upregulated in both cell types under shear stress (Figure 18). They also showed similarities in the cardio-protective genes SOD-1, which was down regulated, and EDN-1, which was upregulated (Figure 19). The coagulation and fibrinolysis genes were both down regulated for HCAECs and upregulated in HUVECs (Figure 20).

In addition to gene expression, levels of nitrates in the media were measured. ECs synthesize and release vasodilators: nitric oxide (NO), prostacyclin and adenosine, which are counteracted in a constant balance with other vasoconstrictor such as endothelin-1. NO is derived from L-arginine by the action of nitric oxide synthase (NOS). Endothelial NOS (eNOS) has a constitutive expression and it generates small amounts of NO for short periods (Nathan and Xie, 1994). In the model of the current study, there is an inversely proportional trend in eNOS production and Nitrate/Nitrite released to the media (Figure 24). When eNOS reaches its peak at 0.3 Pa, the lowest value of Nitrates/Nitrites is present in the media for HCAECs. Similarly, when eNOS reaches the lowest expression at 1.2 Pa, more Nitrates/Nitrites are released into the medium. The downregulation of eNOS at 1.2 Pa suggests that eNOS is not constitutively expressed at this intensity. Moreover, NO should be in balance with EDN-1, however, Figure 19 shows that EDN-1 was down regulated in every condition.

Inhibition of CCL7 would simultaneously lead to lower chronic inflammation, as well as protect the ECs from the environmental metabolic stress (Dahinden, 1994). Over time, this will improve vascular health protecting T2DM patients from arterial complications. One ambitious goal was to design CRISPRs and target 1016 iPSCs-ECs, which would be further differentiated into ECs. Both the genome editing as well as the differentiation techniques have been established over previous years as powerful systems amenable to disease modeling using iPS *in vitro*. Despite the advantages of these technologies and the progress made here, our allotted time was not sufficient to conclude this part of the project. Even though we could generate a knock out for CCL7, there was not enough time to successfully create knock out mutants. Unfortunately, cells died during the expansion step and it was decided to stop the experiment at this point.

My system set up (Figure 11) had a few limitations. First of all, the pump consisted of three valves and only three different shear stress intensities were able to run simultaneously. The second problem that I encountered was that the six channel chip that was designed for me, was designed in a manner that the nozzles would not be stable. This caused the

system to leak and impaired the use of this chip. The last limitation was that the 1016 iPSC-ECs were more delicate and susceptible than the HCAECs and their viability in the camber was low. qPCR results show that expression was very low for most of the tested genes, probably due to the low DNA concentration (Figure 23). Gene expression in 1016 iPSC-ECs appears to be inconsistent in comparison with HCAECs. This could be due to the low viability of the 1016 iPSC-ECs inside the chamber and their susceptibility to media change. They also appear to be sensitive to confluency, causing apoptosis. This should be taken in account when repeating the shear stress experiment with 1016 iPSC-ECs. The new experiment should be conducted for only 24 hours instead of 48 hours and the seeding density should be between the two that were tested ($5x10^6$ – $1x10^7$).

A novel method to improve disease modeling would be to combine shear stress with co-culture. Recent studies are even performed with the two parameters. Yeh et al. (2011) successfully developed a system were they co-cultured ECs and VSMCs and studied their migration under shear stress. They found that shear stress have a great influence on cell migration.

5 Conclusion

My thesis examined the effects of shear stress on ECs and its potential relation with CVD. In order to better understand the mechanism CVD, a better system to represent vascular system in human body was investigated and additionally, the role of shear stress in pro-inflammatory protein production, endothelial adhesion molecules expression and vascular constrictor factors related to coagulation-fibrinolysis.

The main finding of this study is that mRNA expressions in ECs including KRIT-1 and ENG showed completely different expression levels depending on the shear pressure compared to static flow. This demonstrated that the disease model using ECs in petri-dish can be limited to study disease models.

The advantages of using hiPSC-dECs are their applicability to novel cell therapy. Our research sought to suggest a novel avenue for prevention of shear stress related vascular pathology. Although the expression levels of genes in hiPSC-dECs were different from primary ECs, it still remains as good strategy for novel therapy.

Bibliography

Alberti, K. and Zimmet, P. (1998). Definition, diagnosis and classification of diabetes mellitus and its complications. Part 1: diagnosis and classification of diabetes mellitus. Provisional report of a WHO Consultation. *Diabet. Med.*, 15(7), pp.539-553.

Allender S, Scarborough P, Peto V, Rayner M, Leal J, Luengo-Fernandez R, et al. European cardiovascular disease statistics. Brussels: European Heart Network 2008.

Avior, Y., Sagi, I. and Benvenisty, N. (2016). Pluripotent stem cells in disease modelling and drug discovery. *Nature Reviews Molecular Cell Biology*, 17(3), pp.170-182.

Barrangou, R. (2012). RNA-mediated programmable DNA cleavage. *Nat Biotechnol*, 30(9), pp.836-838.

Berliner, J. and Heinecke, J. (1996). The role of oxidized lipoproteins in atherogenesis. *Free Radical Biology and Medicine*, 20(5), pp.707-727.

Berg, J. (2003). Hereditary haemorrhagic telangiectasia: a questionnaire based study to delineate the different phenotypes caused by endoglin and ALK1 mutations. *Journal of Medical Genetics*, 40(8), pp.585-590.

Bhattacharya, S., Dey, D. and Roy, S. (2007). Molecular mechanism of insulin resistance. *J Biosci*, 32(2), pp.405-413.

Bhaya, D., Davison, M. and Barrangou, R. (2011). CRISPR-Cas Systems in Bacteria and Archaea: Versatile Small RNAs for Adaptive Defense and Regulation. *Annu. Rev. Genet.*, 45(1), pp.273-297.

Bibikova, M., Carroll, D., Segal, D., Trautman, J., Smith, J., Kim, Y. and Chandrasegaran, S. (2001). Stimulation of Homologous Recombination through Targeted Cleavage by Chimeric Nucleases. *Molecular and Cellular Biology*, 21(1), pp.289-297.

Bouïs, D., Hospars, G.A:P., Meijer, C., Molema, G. And Mulder, N. (2001) Endothelium in vitro: A review of human vascular endothelial cell lines for blood vessel-related research. *Angiogenesis,* 4(2), pp. 91-102.

Braverman, I., Keh, A. and Jacobson, B. (1990). Ultrastructure and Three-Dimensional Organization of the Telangiectases of Hereditary Hemorrhagic Telangiectasia. *Journal of Investigative Dermatology*, 95(4), pp.422-427.

Cathomen, T. and Keith Joung, J. (2008). Zinc-finger Nucleases: The Next Generation Emerges. *Mol Ther*, 16(7), pp.1200-1207.

Challet Meylan, L., Patsch, C. and Thoma, E. (2015). Endothelial cells differentiation from hPSCs. *Protocol Exchange*.

Chandrasegaran, S. and Smith, J. (1999). Chimeric Restriction Enzymes: What Is Next?. *Biological Chemistry*, 380(7-8).

Chang, L., Chiang, S.H. and Saltiel A.R. (2004). Insulin Signaling and the Regulation of Glucose Transport. *Molecular Medicine,* 10(7-12), pp. 65-71.

Chetty, S., Pagliuca, F., Honore, C., Kweudjeu, A., Rezania, A. and Melton, D. (2013). A simple tool to improve pluripotent stem cell differentiation. *Nature Methods*, 10(6), pp.553-556.

Chiu, Y., Kusano, K., Thomas, T. and Fujiwara, K. (2004). Endothelial Cell-Cell Adhesion and Mechanosignal Transduction. *Endothelium*, 11(1), pp.59-73.

Cong, L., Ran, F., Cox, D., Lin, S., Barretto, R., Habib, N., Hsu, P., Wu, X., Jiang, W., Marraffini, L. and Zhang, F. (2013). Multiplex Genome Engineering Using CRISPR/Cas Systems. *Science*, 339(6121), pp.819-823.

Dahinden, C. (1994). Monocyte chemotactic protein 3 is a most effective basophil- and eosinophil-activating chemokine. *Journal of Experimental Medicine*, 179(2), pp.751-756.

Deng, D., Yan, C., Pan, X., Mahfouz, M., Wang, J., Zhu, J., Shi, Y. and Yan, N. (2012). Structural Basis for Sequence-Specific Recognition of DNA by TAL Effectors. *Science*, 335(6069), pp.720-723.

Deltcheva, E., Chylinski, K., Sharma, C., Gonzales, K., Chao, Y., Pirzada, Z., Eckert, M., Vogel, J. and Charpentier, E. (2011). CRISPR RNA maturation by trans-encoded small RNA and host factor RNase III. *Nature*, 471(7340), pp.602-607.

De Val, S. and Black, B. (2009). Transcriptional Control of Endothelial Cell Development. *Developmental Cell*, 16(2), pp.180-195.

Dimmeler, S., Hermann, C., Galle, J. and Zeiher, A. (1999). Upregulation of Superoxide Dismutase and Nitric Oxide Synthase Mediates the Apoptosis-Suppressive Effects of Shear Stress on Endothelial Cells. *Arteriosclerosis, Thrombosis, and Vascular Biology*, 19(3), pp.656-664.

Ding, Q., Lee, Y., Schaefer, E., Peters, D., *et al.* (2013). A TALEN Genome-Editing System for Generating Human Stem Cell-Based Disease Models. *Cell Stem Cell*, 12(2), pp.238-251.

Engelhardt, B. and Ransohoff, R. (2012). Capture, crawl, cross: the T cell code to breach the blood–brain barriers. *Trends in Immunology*, 33(12), pp.579-589.

Fuster, V., Poon, M. and Willerson, J. (1998). Learning From the Transgenic Mouse : Endothelium, Adhesive Molecules, and Neointimal Formation. *Circulation*, 97(1), pp.16-18.

Gaj, T., Gersbach, C. and Barbas, C. (2013). ZFN, TALEN, and CRISPR/Cas-based methods for genome engineering. *Trends in Biotechnology*, 31(7), pp.397-405.

Gawaz, M. (2005). Platelets in inflammation and atherogenesis. *Journal of Clinical Investigation*, 115(12), pp.3378-3384.

Granger, D. and Senchenkova, E. (2010). *Inflammation and the microcirculation*. [San Rafael, CA]: Morgan & Claypool Life Sciences Publishers.

Gutschner, T., Baas, M. and Diederichs, S. (2011). Noncoding RNA gene silencing through genomic integration of RNA destabilizing elements using zinc finger nucleases. *Genome Research*, 21(11), pp.1944-1954.

Haffner, S., Lehto, S., Rönnemaa, T., Pyörälä, K. and Laakso, M. (1998). Mortality from Coronary Heart Disease in Subjects with Type 2 Diabetes and in Nondiabetic Subjects with and without Prior Myocardial Infarction. *New England Journal of Medicine*, 339(4), pp.229-234.

Helgadottir, A., Thorleifsson, G., Magnusson, K., et al. (2008). The same sequence variant on 9p21 associates with myocardial infarction, abdominal aortic aneurysm and intracranial aneurysm. *Nature Genetics*, 40(2), pp.217-224.

Helgadottir, A., Thorleifsson, G., Manolescu, A., et al. (2007). A Common Variant on Chromosome 9p21 Affects the Risk of Myocardial Infarction. *Obstetrical & Gynecological Survey*, 62(9), pp.585-587.

Hussain, K., Challis, B., Rocha, N., *et al*. (2011). An Activating Mutation of AKT2 and Human Hypoglycemia. *Science*, 334(6055), pp.474-474.

Huo, Y., Hafezi-Moghadam, A. and Ley, K. (2000). Role of Vascular Cell Adhesion Molecule-1 and Fibronectin Connecting Segment-1 in Monocyte Rolling and Adhesion on Early Atherosclerotic Lesions. *Circulation Research*, 87(2), pp.153-159.

Jain, R. (2003). Molecular regulation of vessel maturation. *Nature Medicine*, 9(6), pp.685-693.

Jankele, R. and Svoboda, P. (2014). TAL effectors: tools for DNA Targeting. *Briefings in Functional Genomics*, 13(5), pp.409-419.

Jensen, N., Dalsgaard, T., Jakobsen, M., Nielsen, R., Sørensen, C., Bolund, L. and Jensen, T. (2011). An update on targeted gene repair in mammalian cells: methods and mechanisms. *J Biomed Sci*, 18(1), p.10.

Jinek, M., Chylinski, K., Fonfara, I., Hauer, M., Doudna, J. and Charpentier, E. (2012). A Programmable Dual-RNA-Guided DNA Endonuclease in Adaptive Bacterial Immunity. *Science*, 337(6096), pp.816-821.

Khan, B., Parthasarathy, S., Alexander, R. and Medford, R. (1995). Modified low density lipoprotein and its constituents augment cytokine-activated vascular cell adhesion molecule-1 gene expression in human vascular endothelial cells. *Journal of Clinical Investigation*, 95(3), pp.1262-1270.

Khan, O. and Sefton, M. (2010). Endothelial cell behaviour within a microfluidic mimic of the flow channels of a modular tissue engineered construct. *Biomedical Microdevices*, 13(1), pp.69-87.

Kahn, S., Cooper, M. and Del Prato, S. (2014). Pathophysiology and treatment of type 2 diabetes: perspectives on the past, present, and future. *The Lancet*, 383(9922), pp.1068-1083.

Karvelis, T., Gasiunas, G., Miksys, A., Barrangou, R., Horvath, P. and Siksnys, V. (2013). crRNA and tracrRNA guide Cas9-mediated DNA interference inStreptococcus thermophilus. *RNA Biology*, 10(5), pp.841-851.

Laurindo, F., Pedro M de, A., Barbeiro, H., Pileggi, F., Carvalho, M., Augusto, O. and da Luz, P. (1994). Vascular free radical release. Ex vivo and in vivo evidence for a flow-dependent endothelial mechanism. *Circulation Research*, 74(4), pp.700-709.

LeRoith, D., Quon, M.J. and Zick, Y. (2003). Molecular and cellular aspects of insulin resistance: Implications in diabetes. In: Siganl Transduction and human disease. Editor: Finkel T, Gutkind, JS Hoboken, New Jersey Wiley-Interscience, pp 171-200.

Lopes-Virella, M. and Virella, G. (1996). Modified Lipoproteins, Cytokines and Macrovascul Disease in Non-insulin-dependent Diabetes Mellitus. *Annals of Medicine*, 28(4), pp.347-354.

Lovelace, M., Yap, M., Yip, J., Muller, W., Wijburg, O. and Jackson, D. (2013). Absence of Platelet Endothelial Cell Adhesion Molecule 1, PECAM-1/CD31, In Vivo Increases Resistance to Salmonella enterica Serovar Typhimurium in Mice. *Infection and Immunity*, 81(6), pp.1952-1963.

Luscinskas, F.W. and Lawler, J. (1994). Integrins as dynamic regulators of vascular function. *FASEB journal,* 8(12), pp.929-38.

Makarova, KS., Grishin, NV., Shabalina, SA., Wolf, YI. And Koonin, EV. (2006). A putative RNA-interference-based immune system in prokaryotes: computational analysis of the predicted enzymatic machinery, functional analogies with eukaryotic RNAi, and hypothetical mechanisms of action. *Biology direct,* 16, pp.1-7.

MatÉs, J., Pérez-Gómez, C. and De Castro, I. (1999). Antioxidant enzymes and human diseases. *Clinical Biochemistry*, 32(8), pp.595-603.

Matlung, H., Bakker, E. and VanBavel, E. (2009). Shear Stress, Reactive Oxygen Species, and Arterial Structure and Function. *Antioxidants & Redox Signaling*, 11(7), pp.1699-1709.

McPherson, R. (2010). Chromosome 9p21 and Coronary Artery Disease. *New England Journal of Medicine*, 362(18), pp.1736-1737.

McPherson, R., Pertsemlidis, A., Kavaslar, N., Stewart, A., Roberts, R., Cox, D., Hinds, D., Pennacchio, L., Tybjaerg-Hansen, A., Folsom, A., Boerwinklle, E., Hobbs, H. and Cohen, J. (2007). A Common Allele on Chromosome 9 Associated With Coronary Heart Disease. *Obstetrical & Gynecological Survey*, 62(9), pp.584-585.

Melidonis, A., Dimopoulos, V., Lempidakis, E., Hatzissavas, J., Kouvaras, G., Stefanidis, A., Foussas, S. and Foussas, S. (1999). Angiographic Study of Coronary Artery Disease in Diabetic Patients in Comparison with Nondiabetic Patients. *Angiology*, 50(12), pp.997-1006.

Mongrain, R. and Rodés-Cabau, J. (2006). Role of Shear Stress in Atherosclerosis and Restenosis After Coronary Stent Implantation. *Revista Española de Cardiología (English Edition)*, 59(1), pp.1-4.

Nathan, C. and Xie, Q. (1994). Nitric oxide synthases: Roles, tolls, and controls. *Cell*, 78(6), pp.915-918.

Ncbi.nlm.nih.gov. (2016). *EDN1 endothelin 1 [Homo sapiens (human)] - Gene - NCBI*. [online] Available at: http://www.ncbi.nlm.nih.gov/gene/1906 [Accessed 31 Aug. 2016].

Ncbi.nlm.nih.gov. (2016). *PLA2G4C phospholipase A2 group IVC [Homo sapiens (human)] - Gene - NCBI*. [online] Available at: http://www.ncbi.nlm.nih.gov/gene/8605 [Accessed 31 Aug. 2016].

Ncbi.nlm.nih.gov. (2016). *PLAU plasminogen activator, urokinase [Homo sapiens (human)] - Gene - NCBI*. [online] Available at: http://www.ncbi.nlm.nih.gov/gene/5328 [Accessed 31 Aug. 2016].

Ochs, H., Smith, C. and Puck, J. (2007). *Primary immunodeficiency diseases*. New York: Oxford University Press.

Pabo, CO., Peisach, E. And Grant RA. (2001). Design and selection of novel Cys2His2 zinfinger proteins. *Annual Review of Biochemistry*, 70, pp. 313-40.

Pahakis, M., Kosky, J., Dull, R. and Tarbell, J. (2007). The role of endothelial glycocalyx components in mechanotransduction of fluid shear stress. *Biochemical and Biophysical Research Communications*, 355(1), pp.228-233.

Pandey, U. and Nichols, C. (2011). Human Disease Models in Drosophila melanogaster and the Role of the Fly in Therapeutic Drug Discovery. *Pharmacological Reviews*, 63(2), pp.411-436.

Pasmant, E., Laurendeau, I., Heron, D., Vidaud, M., Vidaud, D. and Bieche, I. (2007). Characterization of a Germ-Line Deletion, Including the Entire INK4/ARF Locus, in a Melanoma-Neural System Tumor Family: Identification of ANRIL, an Antisense Noncoding RNA Whose Expression Coclusters with ARF. *Cancer Research*, 67(8), pp.3963-3969.

Patsch, C., Challet-Meylan, L., Thoma, E., et al. (2015). Generation of vascular endothelial and smooth muscle cells from human pluripotent stem cells. *Nature Cell Biology*, 17(8), pp.994-1003.

Privratsky, J., Paddock, C., Florey, O., Newman, D., Muller, W. and Newman, P. (2011). Relative contribution of PECAM-1 adhesion and signaling to the maintenance of vascular integrity. *Journal of Cell Science*, 124(9), pp.1477-1485.

Pyeritz, R. (2000). The Marfan Syndrome. *Annual Review of Medicine*, 51(1), pp.481-510.

Rajavashisth, T., Qiao, J., Tripathi, S., Tripathi, J., Mishra, N., Hua, M., Wang, X., Loussararian, A., Clinton, S., Libby, P. and Lusis, A. (1998). Heterozygous osteopetrotic (op) mutation reduces atherosclerosis in LDL receptor- deficient mice. *Journal of Clinical Investigation*, 101(12), pp.2702-2710.

Rand, J., Wu, X., Quinn, A., Ashton, A., Chen, P., Hathcock, J., Andree, H. and Taatjes, D. (2009). Hydroxychloroquine protects the annexin A5 anticoagulant shield from disruption by antiphospholipid antibodies: evidence for a novel effect for an old antimalarial drug. *Blood*, 115(11), pp.2292-2299.

Renkin, E. and Curry, F. (1982). Endothelial permeability: pathways and modulations. *Ann NY ACVD Sci*, 401(1 Endothelium), pp.248-258.

Robinson, P. (2000). The molecular genetics of Marfan syndrome and related microfibrillopathies. *Journal of Medical Genetics*, 37(1), pp.9-25.

Robinson, P., Booms, P., Katzke, S., Ladewig, M., Neumann, L., Palz, M., Pregla, R., Tiecke, F. and Rosenberg, T. (2002). Mutations of FBN1 and genotype-phenotype correlations in Marfan syndrome and related fibrillinopathies. *Human Mutation*, 20(3), pp.153-161.

Samani, N., Erdmann, J., Hall, A., et al. (2007). Genomewide Association Analysis of Coronary Artery Disease. *New England Journal of Medicine*, 357(5), pp.443-453.

Sata, M. and Walsh, K. (1998). Oxidized LDL activates fas-mediated endothelial cell apoptosis. *Journal of Clinical Investigation*, 102(9), pp.1682-1689.

Schinzel, R., Ahfeldt, T., Lau, F., Lee, Y., Cowley, A., Shen, T., Peters, D., Lum, D. and Cowan, C. (2011). Efficient Culturing and Genetic Manipulation of Human Pluripotent Stem Cells. *PLoS ONE*, 6(12), p.e27495.

Selle, K. and Barrangou, R. (2015). Harnessing CRISPR–Cas systems for bacterial genome editing. *Trends in Microbiology*, 23(4), pp.225-232.

SenBanerjee, S., Lin, Z., Atkins, G., Greif, D., Rao, R., Kumar, A., Feinberg, M., Chen, Z., Simon, D., Luscinskas, F., Michel, T., Gimbrone, M., García-Cardeña, G. and Jain, M. (2004). KLF2 Is a Novel Transcriptional Regulator of Endothelial Proinflammatory Activation. *The Journal of Experimental Medicine*, 199(10), pp.1305-1315.

Sesti, G. (2006). Pathophysiology of insulin resistance. *Best Practice & Research Clinical Endocrinology & Metabolism*, 20(4), pp.665-679.

Shashkin, P., Dragulev, B. and Ley, K. (2005). Macrophage Differentiation to Foam Cells. *CPD*, 11(23), pp.3061-3072.

Silverthorn, D. (2007). *Human physiology*. San Francisco: Pearson/Benjamin Cummings.

Singh, K., Rommel, K., Mishra, A., Karck, M., Haverich, A., Schmidtke, J. and Arslan-Kirchner, M. (2006). TGFBR1 and TGFBR2 mutations in patients with features of Marfan syndrome and Loeys-Dietz syndrome. *Human Mutation*, 27(8), pp.770-777.

Smith, J. (2000). Requirements for double-strand cleavage by chimeric restriction enzymes with zinc finger DNA-recognition domains. *Nucleic Acids Research*, 28(17), pp.3361-3369.

Staal, F. and Clevers, H. (2005). WNT signalling and haematopoiesis: a WNT–WNT situation. *Nat Rev Immunol*, 5(1), pp.21-30.

Stary, H., Chandler, A., Glagov, S., Guyton, J., Insull, W., Rosenfeld, M., Schaffer, S., Schwartz, C., Wagner, W. and Wissler, R. (1994). A definition of initial, fatty streak, and intermediate lesions of atherosclerosis. A report from the Committee on Vascular Lesions of the Council on Arteriosclerosis, American Heart Association. *Circulation*, 89(5), pp.2462-2478.

Sumi, T., Tsuneyoshi, N., Nakatsuji, N. and Suemori, H. (2008). Defining early lineage specification of human embryonic stem cells by the orchestrated balance of canonical Wnt/ -catenin, Activin/Nodal and BMP signaling. *Development*, 135(17), pp.2969-2979.

Sumpio, B., Timothy Riley, J. and Dardik, A. (2002). Cells in focus: endothelial cell. *The International Journal of Biochemistry & Cell Biology*, 34(12), pp.1508-1512.

The American Heritage medical dictionary. (2007). Boston: Houghton Mifflin Co [Accessed 8 Aug. 2016].

Tocris Bioscience. (2016). *Insulin Signaling Pathway | Tocris Bioscience*. [online] Available at: https://www.tocris.com/pathways/insulinPathway.php#key [Accessed 6 Jun. 2016].

Tousoulis, D., Antoniades, C., Vasiliadou, C., Toutouza, M., Marinou, K., Tentolouris, C., Pitsavos, C., Vlachopoulos, C., Tsioufis, C. and Stefanadis, C. (2005). The effect of diabetes mellitus type 2, on endothelial function and inflammatory process in patients with coronary artery disease. *American Journal of Hypertension*, 18(5), pp.A245-A245.

Tsou, C. (2001). Tumor Necrosis Factor-alpha -converting Enzyme Mediates the Inducible Cleavage of Fractalkine. *Journal of Biological Chemistry*, 276(48), pp.44622-44626.

Ucd.ie. (2016). *Atherosclerosis | OverPath*. [online] Available at: http://www.ucd.ie/mededtec/overPath/atherosclerosis/ [Accessed 24 Aug. 2016].

Ucuzian, A., Gassman, A., East, A. and Greisler, H. (2010). Molecular Mediators of Angiogenesis. *Journal of Burn Care & Research*, 31(1), pp.158-175.

Uzarski, J., Scott, E. and McFetridge, P. (2013). Adaptation of Endothelial Cells to Physiologically-Modeled, Variable Shear Stress. *PLoS ONE*, 8(2), p.e57004.

Visel, A., Zhu, Y., May, D., Afzal, V., Gong, E., Attanasio, C., Blow, M., Cohen, J., Rubin, E. and Pennacchio, L. (2010). Targeted deletion of the 9p21 non-coding coronary artery disease risk interval in mice. *Nature*, 464(7287), pp.409-412.

Wang, H., Yang, H., Shivalila, C., Dawlaty, M., Cheng, A., Zhang, F. and Jaenisch, R. (2013). One-Step Generation of Mice Carrying Mutations in Multiple Genes by CRISPR/Cas-Mediated Genome Engineering. *Cell*, 153(4), pp.910-918.

Whitehead, K., Smith, M. and Li, D. (2012). Arteriovenous Malformations and Other Vascular Malformation Syndromes. *Cold Spring Harbor Perspectives in Medicine*, 3(2), pp.a006635-a006635.

World Health Organization. (2016). *Cardiovascular diseases (CVDs)*. [online] Available at: http://www.who.int/mediacentre/factsheets/fs317/en/ [Accessed 4 Aug. 2016].

Yeh, C., Tsai, S., Wu, L. and Lin, Y. (2011). Using a co-culture microsystem for cell migration under fluid shear stress. *Lab on a Chip*, 11(15), p.2583.

Young, E., Wheeler, A. and Simmons, C. (2007). Matrix-dependent adhesion of vascular and valvular endothelial cells in microfluidic channels. *Lab on a Chip*, 7(12), p.1759.

Zaragoza, C., Gomez-Guerrero, C., Martin-Ventura, J., Blanco-Colio, L., Lavin, B., Mallavia, B., Tarin, C., Mas, S., Ortiz, A. and Egido, J. (2011). Animal Models of Cardiovascular Diseases. *Journal of Biomedicine and Biotechnology*, 2011, pp.1-13.

Zetsche, B., Gootenberg, J., Abudayyeh, O., Slaymaker, I., Makarova, K., Essletzbichler, P., Volz, S., Joung, J., van der Oost, J., Regev, A., Koonin, E. and Zhang, F. (2015). Cpf1 Is a Single RNA-Guided Endonuclease of a Class 2 CRISPR-Cas System. *Cell*, 163(3), pp.759-771.

List of Figures

List of Tables

List of Abbreviations

1016 iPSC-ECs	1016 iPSC derived ECs
Aas	Amino acids
Akt	Protein kinase B
AKT2	Akt2 gene
AKT2 E17K	Clone with a missense mutation in *AKT2* at pGlu17Lys
AKT2 KO	KO mutation clone of *AKT2*
AKT2 WT	Wild type clone from *AKT2* targeting
Cas9	CRISPR associated protein 9
CCL7	Chemokine (C-C motif) ligand 7
cr-RNA	CRISPR RNA
CRISPR	Clustered regularly interspaced short Palindromic Repeats
CVD	Cardiovascular Disorder
DSB	Double-strand break
EC/ECs	Endothelial cell(s)
EDN-1	Endothelin-1
ENG	Endoglin
eNOS	Endothelial NOS
ERK1/2	Extracellular signal-regulated kinase 1/2
FACS	Fluorescence-activated cell sorting
GFP	Green Fluorescence Protein
gRNA	Guide RNA
GWAS	Genome-wide associated studies
HCAEC	Human Coronary Artery Endothelial Cell
HEK 293 T	Human Embryonic Kidney 293 T cells
HHT	Hereditary hemorrhagic telangiectasia
hPSC/hPSCs	Human pluripotent stem cell(s)
hPSC-ECs	hPSC-derived ECs
HR	Homologous recombination
HUVEC	Human Umbilical Vein Endothelial cell
ICAM-1	Intercellular adhesion molecule-1
IL-8	Interleukin 8
iPSC/iPSCs	Induced pluripotent stem cell(s)
IR	Insulin receptor
IRS	Insulin receptor substrate
KLF2	Kruppel-like factor 2
LDL	Low density lipid
LFA 1	Leukocyte Function-associated Antigen 1
lncRNA	Long non-coding RNA

LPS	Lipopolysaccharide
Mac 1	Macrophage 1 antigen
MACS	Magnetic-activated cell sorting
MAP kinase	Mitogen-activated protein kinase
NAPDH	Nicotinamide adenine dinucleotide phosphate
NHEJ	Non-homologous end joining
NO	Nitric oxide
NOS	NO synthase
PAF	Platelet activating factor
PAM	Protospacer Associated Motif
PECAM	Platelet endothelial cell adhesion molecule (CD31)
PI3K	Phosphoinositide 3-kinase
RVD	Repeat Variable Diresidue
Ser/Thr	Serine/threonine
Sev-A 1016	Human sendai viral 1016 iPSC line
SNP	Single nucleotide polymorphism
SOD-1	Superoxide dismutase-1
T1DM	Type 1 Diabetes Mellitus
T2DM	Type 2 Diabetes Mellitus
TALEN	Transcription activator-like effector nuclease
TGFβ	Transforming growth factor β
TGFβRII	Transforming growth factor β receptor type II
TNF-α	Tumor necrosis factor-α
tracRNA	Trans-activating RNA CRISPR
Tyr	Tyrosine residue
VCAM	Vascular cell adhesion molecule
VE-Cadherin	Vascular endothelial Cadherin 5 (CD-144)
VEGFA	Vascular endothelial growth factor-A
VLA-4	Very Late Antigen-4
vWF	Von Willerbrand factor
ZN	Zinc finger
ZNF	Zinc finger nuclease